receptor antagonist—a review of preclinical data. *Neuropharmacol* 1999;**38**:735–767.

2. Reisberg B, Doody R, Stöffler A, Schmitt F, Ferris S, Möbius HJ. Memantine in moderate-to-severe Alzheimer's disease. *N Engl J Med* 2003;**348**:1333–1341.

3. Hare WA, WoldeMussie E, Weinreb RN, Ton H, Ruiz G, Wijono M, Feldmann B, Zangwill L, Wheeler L. Efficacy and safety of memantine treatment for reduction of changes associated with experimental glaucoma in monkey, II: Structural measures. *Invest Ophthalmol Vis Sci* 2004;**45**:2640–2651.

4. Quigley HA. Number of people with glaucoma worldwide. *Br J Ophthalmol* 1996;**80**:389–393.

5. Yücel YH, Gupta N, Zhang Q, Mizisin AP, Kalichman MW, Weinreb RN. Memantine protects neurons from shrinkage in the lateral geniculate nucleus in experimental glaucoma. *Arch Ophthalmol* 2006;**124**:217–225.

6. Dreyer EB, Zurakowski D, Schumer RA, Podos SM, Lipton SA. Elevated glutamate levels in the vitreous body of humans and monkeys with glaucoma. *Arch Ophthalmol* 1996;**114**:299–305.

7. Honkanen RA, Baruah S, Zimmerman MB, Khanna CL, Weaver YK, Narkiewicz J, Waziri R, Gehrs KM, Weingeist TA, Boldt HC, Folk JC, Russell SR, Kwon YH. Vitreous amino acid concentrations in patients with glaucoma undergoing vitrectomy. *Arch Ophthalmol* 2003;**121**:183–188.

8. Lipton SA, Rosenberg PA. Excitatory amino acids as a final common pathway for neurologic disorders. *N Engl J Med* 1994;**330**:613–622.

9. Osborne NN, Wood JP, Chidlow G, Bae JH, Melena J, Nash MS. Ganglion cell death in glaucoma: What do we really know? *Br J Ophthalmol* 1999;**83**:980–986.

10. Nakazawa T, Shimura M, Endo S, Takahashi H, Mori N, Tamai M. *N*-Methyl-ᴅ-aspartic acid suppresses Akt activity through protein phosphatase in retinal ganglion cells. *Mol Vis* 2005;**11**:1173–1182.

11. Yoneda S, Tanihara H, Kido N, Honda Y, Goto W, Hara H, Miyawaki N. Interleukin-1beta mediates ischemic injury in the rat retina. *Exp Eye Res* 2001;**73**:661–667.

12. Shimazawa M, Inokuchi Y, Ito Y, Murata H, Aihara M, Miura M, Araie M, Hara H. Involvement of ER stress in retinal cell death. *Mol Vis* 2007;**13**:578–587.

13. Suemori S, Shimazawa M, Kawase K, Satoh M, Nagase H, Yamamoto T, Hara H. Metallothionein, an endogenous antioxidant, protects against retinal neuron damage in mice. *Invest Ophthalmol Vis Sci* 2006;**47**:3975–3982.

14. Ito Y, Shimazawa M, Inokuchi Y, Fukumitsu H, Furukawa S, Araie M, Hara H. Degenerative alterations in the visual pathway after NMDA-induced retinal damage in mice. *Brain Res* 2008;**1212**:89–101.

15. Wang X, Sam-Wah Tay S, Ng YK. Nitric oxide, microglial activities and neuronal cell death in the lateral geniculate

nucleus of glaucomatous rats. *Brain Res* 2000;**878**:136–147.

16. Yücel YH, Zhang Q, Gupta N, Kaufman PL, Weinreb RN. Loss of neurons in magnocellular and parvocellular layers of the lateral geniculate nucleus in glaucoma. *Arch Ophthalmol* 2000;**118**:378–384.

17. Quigley HA, Dunkelberger GR, Green WR. Retinal ganglion cell atrophy correlated with automated perimetry in human eyes with glaucoma. *Am J Ophthalmol* 1989;**107**:453–464.

18. Gupta N, Ang LC, Noel de TL, Bidaisee L, Yücel YH. Human glaucoma and neural degeneration in intracranial optic nerve, lateral geniculate nucleus, and visual cortex. *Br J Ophthalmol* 2006;**90**:674–678.

19. Mooney SM, Miller MW. Postnatal generation of neurons in the ventrobasal nucleus of the rat thalamus. *J Neurosci* 2007;**27**:5023–5032.

20. Kornhuber J, Quack G. Cerebrospinal fluid and serum concentrations of the N-methyl-ᴅ-aspartate (NMDA) receptor antagonist memantine in man. *Neurosci Lett* 1995;**195**:137–139.

21. Zajaczkowski W, Quack G, Danysz W. Infusion of (+)-MK-801 and memantine – contrasting effects on radial maze learning in rats with entorhinal cortex lesion. *Eur J Pharmacol* 1996;**296**:239–246.

22. Minkeviciene R, Banerjee P, Tanila H. Memantine improves spatial learning in a transgenic mouse model of Alzheimer's disease. *J Pharmacol Exp Ther* 2004;**311**:677–682.

23. Vorwerk CK, Lipton SA, Zurakowski D, Hyman BT, Sabel BA, Dreyer EB. Chronic low-dose glutamate is toxic to retinal ganglion cells. Toxicity blocked by memantine. *Invest Ophthalmol Vis Sci* 1996;**37**:1618–1624.

24. Harada T, Harada C, Nakamura K, Quah HM, Okumura A, Namekata K, Saeki T, Aihara M, Yoshida H, Mitani A, Tanaka K. The potential role of glutamate transporters in the pathogenesis of normal tension glaucoma. *J Clin Invest* 2007;**117**:1763–1770.

25. Grunert U, Haverkamp S, Fletcher EL, Wassle H. Synaptic distribution of ionotropic glutamate receptors in the inner plexiform layer of the primate retina. *J Comp Neurol* 2002;**447**:138–151.

26. Vrabec JP, Levin LA. The neurobiology of cell death in glaucoma. *Eye* 2007;**21**(Suppl 1): S11–S14.

27. Finn JT, Weil M, Archer F, Siman R, Srinivasan A, Raff MC. Evidence that Wallerian degeneration and localized axon degeneration induced by local neurotrophin deprivation do not involve caspases. *J Neurosci* 2000;**20**:1333–1341.

28. Jaubert-Miazza L, Green E, Lo FS, Bui K, Mills J, Guido W. Structural and functional composition of the developing retinogeniculate pathway in the mouse. *Vis Neurosci* 2005;**22**:661–676.

29. Jones EG, Tighilet B, Tran BV, Huntsman MM. Nucleus- and cell-specific expression of NMDA and non-NMDA

receptor subunits in monkey thalamus. *J Comp Neurol*
1998;**397**:371–393.

30. Marvanova M, Lakso M, Pirhonen J, Nawa H, Wong G,
    Castren E. The neuroprotective agent memantine
    induces brain-derived neurotrophic factor and trkB
    receptor expression in rat brain. *Mol Cell Neurosci*
    2001;**18**:247–258.

31. Meisner F, Scheller C, Kneitz S, Sopper S, Neuen-Jacob
    E, Riederer P, Meulen VT, Koutsilieri E. Memantine
    upregulates BDNF and prevents dopamine deficits in
    SIV-infected macaques: A novel pharmacological action
    of memantine. *Neuropsychopharmacology*
    2008;**33**:2228–2236.

32. Yücel YH, Yeung J, Weinreb RN, Kaufman PL, Gupta N.
    Alteration of nerve growth factor receptors TrkB and
    TrkC in the lateral geniculate nucleus. Paper presented at
    Annual Association for Research in Vision and
    Ophthalmology Meeting, May 4, Fort Lauderdale, FL,
    2002.

33. Avwenagha O, Bird MM, Lieberman AR, Yan Q,
    Campbell G. Patterns of expression of brain-derived
    neurotrophic factor and tyrosine kinase B mRNAs and
    distribution and ultrastructural localization of their
    proteins in the visual pathway of the adult rat.
    Neuroscience 2006;**140**:913–928.

34. Hetman M, Kanning K, Cavanaugh JE, Xia Z.
    Neuroprotection by brain-derived neurotrophic factor is
    mediated by extracellular signal-regulated kinase and
    phosphatidylinositol 3-kinase. *J Biol Chem*
    1999;**274**:22569–22580.

35. Nakazawa T, Tamai M, Mori N. Brain-derived
    neurotrophic factor prevents axotomized retinal ganglion
    cell death through MAPK and PI3K signaling pathways.
    Invest Ophthalmol Vis Sci 2002;**43**:3319–3326.

ELSEVIER

Combination effects of normobaric hyperoxia and edaravone on focal cerebral ischemia-induced neuronal damage in mice

Yuko Nonaka [a,b], Masamitsu Shimazawa [a], Shinichi Yoshimura [b], Toru Iwama [b], Hideaki Hara [a,*]

[a] Department of Biofunctional Evaluation, Molecular Pharmacology, Gifu Pharmaceutical University, 5-6-1 Mitahora-higashi, Gifu 502-8585, Japan
[b] Departments of Neurosurgery, Gifu University Graduate School of Medicine, 1-1 Yanagido, Gifu 501-1194, Japan

ARTICLE INFO

ABSTRACT

We evaluated the potential neuroprotective effects of combination treatment with normobaric hyperoxia (NBO) and edaravone, a potent scavenger of hydroxyl radicals, on acute brain injuries after stroke. Mice subjected to 2-h filamental middle cerebral artery occlusion were treated with NBO (95% O_2, during the ischemia) alone, with edaravone (1.5 mg/kg, intravenously after the ischemia) alone, with both of these treatments (combination), or with vehicle. The histological and neurological score were assessed at 22-h after reperfusion. Infarct volume was significantly reduced in the combination group [36.3 ± 6.7 mm^3 ($n = 10$) vs. vehicle: 65.5 ± 5.9 mm^3 ($n = 14$) $P < 0.05$], but not in the two monotherapy-groups [NBO: 50.5 ± 5.8 mm^3 ($n = 14$) and edaravone: 56.7 ± 5.8 mm^3 ($n = 10$)]. The combination therapy reduced TUNEL-positive cells in the ischemic boundary zone both in cortex [$6.0 \pm 1.4 \times 10^2$/mm^2 ($n = 5$) vs. vehicle: $18.9 \pm 2.4 \times 10^2$/mm^2 ($n = 5$), $P < 0.01$] and subcortex [$11.6 \pm 1.5 \times 10^2$/mm^2 ($n = 5$) vs. vehicle: $22.5 \pm 2.1 \times 10^2$/mm^2 ($n = 5$), $P < 0.01$]. NBO and combination groups exhibited significantly reduced neurological deficit scores at 22-h after reperfusion (vs. vehicle, $P < 0.05$). Combination therapy with NBO plus edaravone prevented the neuronal damage after focal cerebral ischemia and reperfusion in mice, compared with monotherapy of NBO or edaravone.

© 2008 Elsevier Ireland Ltd. All rights reserved.

Normobaric hyperoxia (NBO), which has the advantage of minimal technical demands, was protective in recent experimental and clinical pilot studies as well [9,14–16]. Moreover, some of the mechanisms of protection by oxygen therapy are beginning to be elucidated. Shin et al. have reported that administration of 100% O_2 prevented the expansion of the zone with a severe cerebral blood flow deficit occurring during distal middle cerebral artery (MCA) occlusion in mice [13]. A phase II study to assess the therapeutic potential of NBO given within 9 h of stroke onset is underway in the USA (Massachusetts General Hospital and National Institute of Neurological Disorders and Stroke).

Edaravone, a potent scavenger of hydroxyl radicals, has been proven to be beneficial for patients with acute ischemic stroke in Japan as well as in rodent models of ischemia [1,8,18]. In a rat transient cerebral ischemia model, edaravone prevented cortical edema, reduced the infarct volume, and improved neurological deficits [2,8]. Qi et al. have showed previously in mice that treatment with edaravone dose-dependently reduced infarction volume and hemispheric swelling, and effective doses for acute ischemia

are from 3 to 10 mg/kg (no significant reduction in infarct volume was observed dosed with 1 mg/kg) [12]. Moreover, Zhang et al. have demonstrated that the combination therapy of edaravone plus tissue plasminogen activator (t-PA) was useful for the extension of the therapeutic time window in a rat transient cerebral ischemia model [19].

If combining two low-dose therapies with different neuroprotective actions were found to increase the target effects and reduce the side effects (compared to single therapy at a regular dose), such combination therapy would be beneficial for stroke patients. For the present study, we chose NBO and edaravone, both of which have proved to be safe and effective therapies against ischemia, and for which the experimental evidence indicates different mechanisms of action, and we evaluated the therapeutic effects of combination treatment.

The purpose of this study was, therefore, to examine the potential neuroprotective effects of concurrent treatment with NBO and a suboptimal dose of edaravone on the cerebral infarct size and the neurological deficits present after subjecting mice to a 2-h occlusion of MCA followed by a 22-h reperfusion.

The experimental designs and all procedures were in accordance with the Animal Care Guidelines of the Animal Experimental Committee of Gifu Pharmaceutical University. Male ddY mice (body

* Corresponding author. Tel.: +81 582 37 8596; fax: +81 582 37 8596.
E-mail address: hidehara@gifu-pu.ac.jp (H. Hara).

weight, 24–28 g; Japan SLC Ltd., Shizuoka, Japan) were housed at controlled room temperature (24.5–25.0 °C), with a 12-h light:12-h dark cycle. Mouse food pellets and tap water were provided ad libitum. Edaravone (3-methyl-1-phenyl-2-pyrazolin-5-one) was kindly gifted by Mitsubishi Tanabe Pharma Corporation Co. Ltd. (Osaka, Japan). Mice of the edaravone and combination groups were treated with jugular vain infusion of edaravone at 1.5 mg/kg body weight once: immediately after completion of MCA occlusion. Mice of the vehicle and NBO groups received intravenous (i.v.) infusion of 2.0 ml/kg saline solutions without edaravone at the volume similar to that used in the edaravone and combination groups. The hyperoxia (NBO alone and combination) groups were started to expose hyperoxia within 2 min after completion of MCA occlusion. And hyperoxia groups were removed from the hyperoxia chamber at 5 min before reperfusion. Isoflurane was purchased from Merck Hoei Co. Ltd. (Osaka, Japan), 2,3,5-Triphenyltetrazolium chloride (TTC) was from Sigma–Aldrich Co. (St. Louis, MO, USA), and pentobarbital sodium was from Dainippon Sumitomo Pharma (Osaka, Japan).

Mice were anesthetized with 1.0–1.5% isoflurane in air (21% O_2) via a face mask (Soft Lander; Sin-ei Industry, Saitama, Japan). Focal cerebral ischemia was induced [using an 8-0 nylon monofilament (Ethicon, Somerville, NJ, USA) coated with silicone hardener mixture (Xantopren, Bayer Dental, Osaka, Japan)] via the internal carotid artery, as described by Hara et al. [5]. Any mice with an intracranial hemorrhage and/or without an ischemic brain infarct were excluded.

After completion of the operation, each mouse was immediately (within 1 min) received an i.v. injection of either vehicle or edaravone (1.5 mg/kg), and promptly put in an environmental chamber. The hyperoxia groups (NBO and combination groups) were exposed to 95 ± 1% O_2 in the chamber [regulated by an oxygen controller (PRO-OX110; Reming Bioinstruments Co., Redfield, USA)] throughout a period (10 min) that was set beforehand. And hyperoxia groups were removed from the hyperoxia chamber at 5 min before reperfusion. The oxygen concentration inside the chamber was continuously monitored using the oxygen controller, and carbon dioxide was cleared using soda lime (Nakarai Tesque Co. Kyoto, Japan) placed on the bottom of the chamber. After 2-h ischemia, the mouse was taken out, and underwent reperfusion, all in room-air (21% O_2). The room-air groups (vehicle and edaravone), when in the environmental chamber, were exposed to room-air equivalent gas.

In all animals during surgery and ischemia, the body temperature was maintained between 37.0 and 37.5 °C with the aid of a heating lamp and heating pad. In randomly selected animals, the left femoral artery was cannulated and blood pressure was measured during the preparation. Mean systemic arterial blood pressure (Power Lab; AD Instrument, Nagoya, Japan) was measured for three 5-min periods (starting at 30 min before and after MCA occlusion). Arterial blood gases were sampled just after these vital measurements. The normoxia (vehicle and edaravone) groups received air (21% O_2) via a face mask, while the hyperoxia (NBO and combination) groups received 0.75 l/min of 100% O_2 (which kept O_2 95% in the center of the face mask) during the ischemia. Blood samples of 50 μl were taken at 30 min before and after the induction of ischemia and analyzed for pH, oxygen (PaO$_2$), and carbon dioxide (PaCO$_2$) (i-SAT 300F; i-SAT Corporation, NJ, USA).

Some mice that died due to subarachnoid hemorrhage, pulmonary insufficiency, or asphyxia were eliminated from the study. Mice were tested for neurological deficits just before reperfusion, 22-h after reperfusion, by an observer (Y.N.) who was blind to the animal groups. Scoring was done using the following scale: 0, no observable neurological deficits; 1, failure to extend the right forepaw; 2, circling to the contralateral side; 3, loss of walking or righting reflex, as described by Hara et al. [5].

At 22-h after reperfusion, mice were given an overdose of pentobarbital sodium and then decapitated. The brain was cut into 2-mm-thick coronal block slices. These slices were immersed for 30 min in a 2% solution of TTC in normal saline at 37 °C, and then fixed in 10% phosphate-buffered formalin at 4 °C. TTC reacts with intact mitochondrial respiratory enzymes to generate a bright red color that contrasts with the pale color of the infarction. The caudal face of each slice was photographed (COOLPIX 4500; Nikon, Tokyo, Japan). The unstained areas of the total, cortical, and subcortical infarctions were measured using Image J (http://rsb.info.nih.gov/ij/download/), and the infarction volume per brain (in mm^3) was calculated as in a previous report [4].

In another series, mice under anesthesia were perfused transcardially with saline followed by 4% paraformaldehyde in 0.1 mol/l phosphate buffer (pH 7.4) at 22-h after reperfusion. Then, the brains were post-fixed overnight in the same fixative, and immersed in 30% sucrose solution in the phosphate buffer. The brains were frozen and cut into 20-μm-thick coronal sections from 0.4 to 1.0 mm anterior to bregma (through the anterior commissure) using a cryostat (Leica Instruments, Nussloch, Germany). Concomitantly, we performed terminal deoxynucleotidyl transferase-mediated dUTP nick end-labeling (TUNEL) staining to identify degenerated cells after the above ischemia with the combination therapy, as previously described [10]. The TUNEL assay was performed according to the manufacturer's instructions (Roche Molecular Biochemicals Inc., Mannheim, Germany). To quantify the number of DNA-fragmented cells present after ischemia, the numbers of TUNEL-positive cells in the ischemic boundary zones within cortex and subcortex were counted. This was done in two high-power fields (×400) within each lesion by a masked investigator (Y.N.). Each count was expressed as number/mm^2 ($n = 5$).

Data are presented as means ± S.E.M. Statistical comparisons were made using an analysis of variance (ANOVA) followed by a Student–Newman–Keuls (SNK) test or a non-parametric Kruskal–Wallis test. $P < 0.05$ was considered to indicate statistical significance.

In the two hyperoxia (NBO and the combination) groups, arterial PaO$_2$ values increased approximately 4-fold during the administration of 100% oxygen. The other physiological parameters were not significantly different among the four groups (Table 1). There was no significant difference in mortality after ischemia among the four groups (data not shown).

The infarct tissue was visualized by TTC staining in the ischemic hemisphere (Fig. 1A). Total infarct volume was significantly reduced in the combination group compared with those of vehicle and edaravone groups ($P < 0.05$, Fig. 1B). But there was no significant difference in total infarct volume of the two monotherapy-groups compared with vehicle [vehicle: 65.5 ± 5.9, NBO: 50.5 ± 5.8, edaravone: 56.7 ± 5.8, combination: 36.3 ± 6.7 mm^3 ($n = 10$–14)]. An ischemic lesion was consistently identified affecting cortex and subcortex of the left cerebral hemisphere. A combination treatment significantly reduced infarct volume both in cortex [vs. vehicle and edaravone, $P < 0.01$ and $P < 0.05$, respectively, vehicle: 41.9 ± 4.8, NBO: 29.2 ± 4.7, edaravone: 39.1 ± 5.2, combination: 22.4 ± 5.7 mm^3 ($n = 10$–14)] (Fig. 1C) and subcortex [vs. vehicle and NBO, $P < 0.01$ and $P < 0.05$, respectively, vehicle: 23.6 ± 1.8, NBO: 21.3 ± 1.7, edaravone: 17.6 ± 1.4, combination: 13.9 ± 1.4 mm^3 ($n = 10$–14)] (Fig. 1D).

The ischemic mice showed apparent neurological deficits just before and at 22-h after reperfusion. There was no significant difference in neurological deficit score among the four groups just before reperfusion (data not shown). In contrast, at 22-h after reperfusion the combination group exhibited significantly reduced neurological deficit scores (vs. vehicle, $P < 0.05$) (Fig. 1E).

Table 1
Physiological variables of mice before and after focal cerebral ischemia

Variables	Vehicle	NBO	Edaravone	Combination
MABP (mmHg)				
Before	76.6 ± 4.93	78.6 ± 3.91	87.5 ± 3.50	84.5 ± 1.41
After	79.3 ± 4.14	76.9 ± 3.20	76.8 ± 1.84	78.0 ± 3.22
PaO₂ (mmHg)				
Before	105.0 ± 8.48	102.4 ± 2.50	106.0 ± 6.20	119.0 ± 2.37
After	95.6 ± 6.59	458.2 ± 23.9*	102.4 ± 5.78	463.0 ± 24.1*
PaCO₂ (mmHg)				
Before	35.8 ± 2.52	41.0 ± 2.16	36.6 ± 1.50	41.7 ± 1.10
After	41.5 ± 2.08	43.4 ± 2.38	43.1 ± 1.24	47.2 ± 1.43
PH				
Before	7.35 ± 0.02	7.32 ± 0.01	7.34 ± 0.00	7.34 ± 0.01
After	7.31 ± 0.02	7.31 ± 0.01	7.30 ± 0.01	7.30 ± 0.02

Analysis of variance (ANOVA) followed by Student–Newman–Keuls (SNK) tests. Data are express as mean ± S.E.M. (n = 5). MABP, mean arterial blood pressure; before, 30 min before middle cerebral artery occlusion (MCAO); after, 30 min after MCAO.
* $P < 0.01$ vs. vehicle.

A large number of cells showed strong TUNEL-positive staining on the ischemic side of the brain, but not the contralateral side. The numbers of TUNEL-positive degenerated cells in the ischemic boundary zones within the cerebral cortex (Fig. 2A) and subcortex (Fig. 2B) showed increases at 22-h after reperfusion. The numbers of TUNEL-positive cells were significantly reduced by the combination treatment in cortex [vs. vehicle and edaravone, $P < 0.01$ and $P < 0.05$, respectively, vehicle: 18.9 ± 2.4, NBO: 9.7 ± 0.6, edaravone: 13.2 ± 2.0, combination: $6.0 \pm 1.4 \times 10^2/mm^2$ (n = 5)] (Fig. 2C) and subcortex [vs. vehicle, NBO, and edaravone, $P < 0.01$, $P < 0.01$, and $P < 0.05$, respectively, vehicle: 22.5 ± 2.1, NBO: 18.6 ± 1.6, edaravone: 17.4 ± 1.1, combination: $11.6 \pm 1.5 \times 10^2/mm^2$
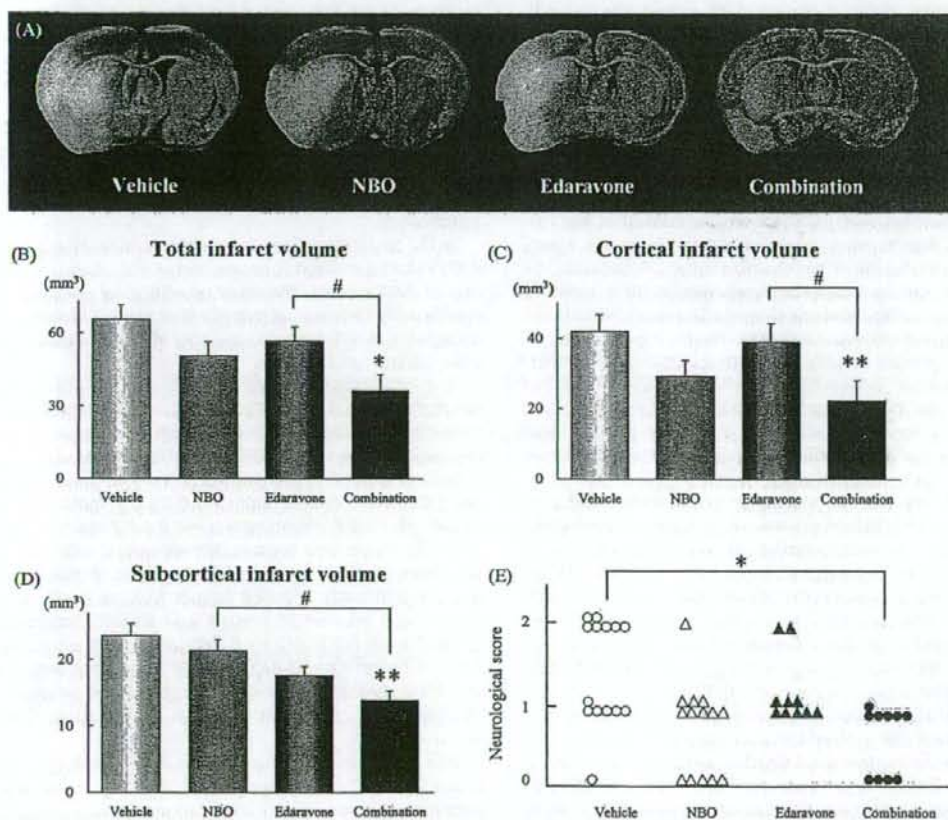

Fig. 1. Infarct volume and neurological deficit scores 22-h after reperfusion. (A) 2,3,5-Triphenyltetrazolium chloride-stained of coronal sections are showing the infarct tissues (pale unstained region). Brain sections (from extreme left) are obtained from vehicle, NBO, edaravone, and combination mice, respectively. Infarct volume of total (B), cortex (C), and subcortex (D). *$P < 0.05$; **$P < 0.01$ vs. vehicle. #Indicates an inter-group difference. Analysis of variance (ANOVA) followed by Student–Newman–Keuls (SNK) tests. (E) Neurological deficit scores. *$P < 0.05$, vs. vehicle (non-parametric Kruskal–Wallis test). Data are expressed as mean ± S.E.M. (n = 10–14).
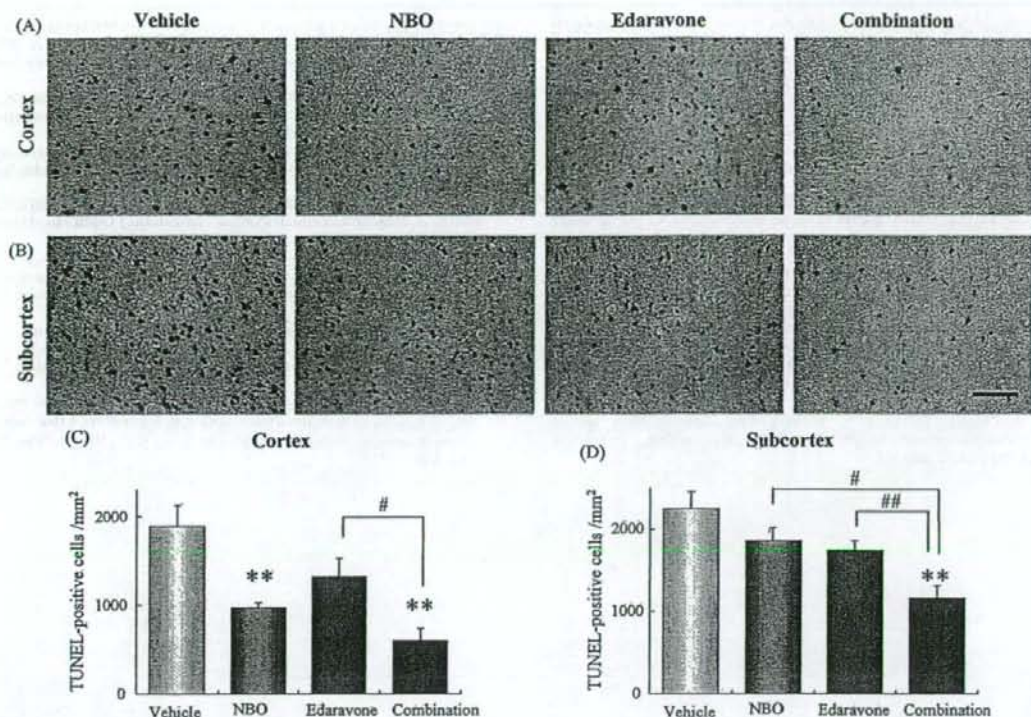
Fig. 2. TUNEL staining induced by 22-h reperfusion. (A and B) show representative photomicrographs of TUNEL staining in the ischemic boundary zones of the cerebral cortex (A) and subcortex (B). Scale bar = 50 μm. Quantitative representation of TUNEL-positive cells in ischemic brains from each group of the cerebral cortex (C) and subcortex (B). ""$P < 0.01$ vs. vehicle. #$P < 0.05$ and ##$P < 0.01$ between indicated groups. Analysis of variance (ANOVA) followed by Student–Newman–Keuls (SNK) tests. Data are expressed as mean ± S.E.M. ($n = 5$).

($n = 5$)] (Fig. 2D). The numbers of TUNEL-positive cells were also significantly reduced by NBO treatment in cortex (vs. vehicle, $P < 0.01$) (Fig. 2C).

In this study, we found that a combination therapy of NBO (95% O_2) during ischemia and a suboptimal dose of edaravone (1.5 mg/kg i.v.) after 2-h MCA occlusion protects functional and morphological outcomes against the ischemic brain in mice. Imai et al. have reported that the hyperbaric oxygen (HBO) therapy combined with intravenous edaravone administration improved the 90-day clinical outcome in patients with acute embolic stroke [7]. From the point of distribution of O_2 to ischemic brain tissue, HBO may have more powerful neuroprotection than NBO to salvage for acute stroke treatment. But various factors such as the limited availability of HBO chambers and poor patient compliance may be difficult for using HBO as the clinical stroke therapy [3]. Previous study indicated that free radicals increased in the blood of humans undergoing HBO therapy [11]. On the other hand, NBO has the advantage of safety and minimal technique, and it can be delivered in an ambulance or even at the patient's home following a stroke. Recent experiments in animals have shown that NBO exerts beneficial effects without increasing markers of oxidative stress [15,16], and a phase II study is underway in the USA, as mentioned above. But theoretical concern remains about reperfusion injury being caused by an increase in oxygen free radicals due to hyperoxia therapy, and oxidative stress reportedly plays a major role in the pathogenesis of the cerebral infarction occurring as a reperfusion injury after focal ischemia [17].

Edaravone has ability to scavenge a variety of free radicals, especially hydroxyl radicals, produced during ischemia/reperfusion

[18]. However, edaravone has some side effects, including acute renal failure, liver dysfunction, and renal dysfunction, during edaravone treatment are occasionally observed. Since death due to acute renal failure during edaravone treatment has been reported, this agent is contraindicated for patients with severe renal dysfunction, and should be carefully used in elderly patients [6]. Further, taking suboptimal dose of drug may reduce the side effect as well as primary aim. The plural therapies for the identical purpose through different mechanisms may be able to get enough effects with minimum risks.

In conclusion, we found that combination therapy with NBO plus edaravone, which have different mechanisms, in spite of each suboptimal dose protected against acute cerebral injury that had undergone focal cerebral ischemia in mice.

References

[1] Edaravone Acute Infarction Study Group. Effect of a novel free radical scavenger, edaravone (MCI-186), on acute brain infarction. Randomized, placebo-controlled, double-blind study at multicenters, Cerebrovasc. Dis. 15 (2003) 222–229.

[2] K. Abe, S. Yuki, K. Kogure, Strong attenuation of ischemic and postischemic brain edema in rats by a novel free radical scavenger, Stroke 19 (1988) 480–485.

[3] D.C. Anderson, A.G. Bottini, W.M. Jagiella, B. Westphal, S. Ford, G.L. Rockswold, R.B. Loewenson, A pilot study of hyperbaric oxygen in the treatment of human stroke, Stroke 22 (1991) 1137–1142.

[4] H. Hara, R.M. Friedlander, V. Gagliardini, C. Ayata, K. Fink, Z. Huang, M. Shimizu-Sasamata, J. Yuan, M.A. Moskowitz, Inhibition of interleukin 1beta converting enzyme family proteases reduces ischemic and excitotoxic neuronal damage, Proc. Natl. Acad. Sci. U.S.A. 94 (1997) 2007–2012.

[5] H. Hara, P.L. Huang, N. Panahian, M.C. Fishman, M.A. Moskowitz, Reduced brain edema and infarction volume in mice lacking the neuronal isoform of nitric

oxide synthase after transient MCA occlusion, J. Cereb. Blood Flow Metab. 16 (1996) 605–611.

[6] Y. Higashi, D. Jitsuiki, K. Chayama, M. Yoshizumi, Edaravone (3-methyl-1-phenyl-2-pyrazolin-5-one), a novel free radical scavenger, for treatment of cardiovascular diseases, Recent Patents Cardiovasc. Drug Discov. 1 (2006) 85–93.

[7] K. Imai, T. Mori, H. Izumoto, N. Takabatake, T. Kunieda, M. Watanabe, Hyperbaric oxygen combined with intravenous edaravone for treatment of acute embolic stroke: a pilot clinical trial, Neurol. Med. Chir. (Tokyo) 46 (2006) 373–378.

[8] H. Kawai, H. Nakai, M. Suga, S. Yuki, T. Watanabe, K.I. Saito, Effects of a novel free radical scavenger, MCI-186, on ischemic brain damage in the rat distal middle cerebral artery occlusion model, J. Pharmacol. Exp. Ther. 281 (1997) 921–927.

[9] H.Y. Kim, A.B. Singhal, E.H. Lo, Normobaric hyperoxia extends the reperfusion window in focal cerebral ischemia, Ann. Neurol. 57 (2005) 571–575.

[10] Y. Kotani, Y. Nakajima, T. Hasegawa, M. Satoh, H. Nagase, M. Shimazawa, S. Yoshimura, T. Iwama, H. Hara, Propofol exerts greater neuroprotection with disodium edetate than without it, J. Cereb. Blood Flow Metab. 28 (2008) 354–366.

[11] C.K. Narkowicz, J.H. Vial, P.W. McCartney, Hyperbaric oxygen therapy increases free radical levels in the blood of humans, Free Radic. Res. Commun. 19 (1993) 71–80.

[12] X. Qi, Y. Okuma, T. Hosoi, Y. Nomura, Edaravone protects against hypoxia/ischemia-induced endoplasmic reticulum dysfunction, J. Pharmacol. Exp. Ther. 311 (2004) 388–393.

[13] H.K. Shin, A.K. Dunn, P.B. Jones, D.A. Boas, E.H. Lo, M.A. Moskowitz, C. Ayata, Normobaric hyperoxia improves cerebral blood flow and oxygenation, and inhibits peri-infarct depolarizations in experimental focal ischaemia, Brain 130 (2007) 1631–1642.

[14] A.B. Singhal, T. Benner, L. Roccatagliata, W.J. Koroshetz, P.W. Schaefer, E.H. Lo, F.S. Buonanno, R.G. Gonzalez, A.G. Sorensen, A pilot study of normobaric oxygen therapy in acute ischemic stroke, Stroke 36 (2005) 797–802.

[15] A.B. Singhal, R.M. Dijkhuizen, B.R. Rosen, E.H. Lo, Normobaric hyperoxia reduces MRI diffusion abnormalities and infarct size in experimental stroke, Neurology 58 (2002) 945–952.

[16] A.B. Singhal, X. Wang, T. Sumii, T. Mori, E.H. Lo, Effects of normobaric hyperoxia in a rat model of focal cerebral ischemia-reperfusion, J. Cereb. Blood Flow Metab. 22 (2002) 861–868.

[17] G. Yang, P.H. Chan, J. Chen, E. Carlson, S.F. Chen, P. Weinstein, C.J. Epstein, H. Kamii, Human copper-zinc superoxide dismutase transgenic mice are highly resistant to reperfusion injury after focal cerebral ischemia, Stroke 25 (1994) 165–170.

[18] N. Zhang, M. Komine-Kobayashi, R. Tanaka, M. Liu, Y. Mizuno, T. Urabe, Edaravone reduces early accumulation of oxidative products and sequential inflammatory responses after transient focal ischemia in mice brain, Stroke 36 (2005) 2220–2225.

[19] W. Zhang, K. Sato, T. Hayashi, N. Omori, I. Nagano, S. Kato, S. Horiuchi, K. Abe, Extension of ischemic therapeutic time window by a free radical scavenger, Edaravone, reperfused with tPA in rat brain, Neurol. Res. 26 (2004) 342–348.

A NOVEL CALPAIN INHIBITOR, ((1S)-1((((1S)-1-BENZYL-3-CYCLOPROPYLAMINO-2,3-DI-OXOPROPYL)AMINO)CARBONYL)-3-METHYLBUTYL) CARBAMIC ACID 5-METHOXY-3-OXAPENTYL ESTER, PROTECTS NEURONAL CELLS FROM CEREBRAL ISCHEMIA-INDUCED DAMAGE IN MICE

A. KOUMURA,[a,b] Y. NONAKA,[a,c] K. HYAKKOKU,[a]
T. OKA,[d] M. SHIMAZAWA,[a] I. HOZUMI,[b] T. INUZUKA[b]
AND H. HARA[a]*

[a]*Department of Biofunctional Evaluation, Molecular Pharmacology, Gifu Pharmaceutical University, 5-6-1 Mitahora-higashi, Gifu 502-5858, Japan*

[b]*Department of Neurology and Geriatrics, Gifu University of Medicine, 1-1 Yahaido, Gifu 501-1194, Japan*

[c]*Department of Neurosurgery, Gifu University of Medicine, 1-1 Yahaido, Gifu 501-1194, Japan*

[d]*Kobe Creative Center, Senju Pharmaceutical Co. Ltd., 1-5-4 Muroya, Nishi-ku, Kobe 651-2241, Japan*

Abstract—Cerebral ischemia induces Ca^{2+} influx into neuronal cells, and activates several proteases including calpains. Since calpains play important roles in neuronal cell death, calpain inhibitors may have potential as drugs for cerebral infarction. ((1S)-1((((1S)-1-Benzyl-3- cyclopropylamino-2,3-di-oxopropyl)amino)carbonyl)-3-methylbutyl) carbamic acid 5-methoxy-3-oxapentyl ester (SNJ-1945) is a novel calpain inhibitor that has good membrane permeability and water solubility. We evaluated the effect of SNJ-1945 on the focal brain ischemia induced by middle cerebral artery occlusion (MCAO) in mice. Brain damage was evaluated by assessing neurological deficits at 24 h or 72 h after MCAO and also by examining 2,3,5-triphenyltetrazolium chloride (TTC) staining and terminal deoxynucleotidyl transferase-mediated dUTP nick-end labeling (TUNEL) staining of brain sections. When injected at 1 h after MCAO, SNJ-1945 at 30 and 100 mg/kg, i.p. decreased the infarction volume and improved the neurological deficits each assessed at 24 h. SNJ-1945 at 100 mg/kg, i.p. also showed neuroprotective effects at 72 h and reduced the number of TUNEL-positive cells at 24 h. SNJ-1945 was able to prevent neuronal cell death even when it was injected at up to 6 h, but not at 8 h, after MCAO. In addition, SNJ-1945 decreased cleaved α-spectrin at 6 h and 12 h, and active caspase-3 at 12 h and 24 h in ischemic brain hemisphere. These findings indicate that SNJ-1945 inhibits the activation of calpain, and offers neuroprotection against the effects of acute cerebral ischemia in mice even when given up to 6 h after MCAO. SNJ-1945 may therefore be a potential drug for stroke. © 2008 IBRO. Published by Elsevier Ltd. All rights reserved.

Calcium ion is a major intracellular messenger, and Ca^{2+} influx regulates synaptic activity, membrane excitability, exocytosis, and enzyme activation (Camins et al., 2006). Although such signals are necessary for cell survival, Ca^{2+}-overload triggers apoptosis via activation of caspases (Bano and Nicotera, 2007).

Calpains are members of the cysteine protease family activated by Ca^{2+}. Fifteen types of calpain have been reported (Camins et al., 2006), but in mammals, calpain I (μ-calpain) and calpain II (m-calpain) are thought to be the most widely distributed. A large number of proteins have been identified as calpain substrates, such as cytoskeletal proteins and proteases (Croall and Ersfeld, 2007). Calpains play important roles in both physiological and pathological processes (Sorimachi et al., 1997; Bertipaglia and Carafoli, 2007), but in particular are known to play roles in neuronal cell death. Calpains cleave pro-caspase-3 to its active form (Camins et al., 2006). Moreover, calpains mediate p53 activation, and indirectly influence release of both cytochrome C and apoptosis-inducing factor (AIF) (Sedarous et al., 2003; Sanges and Marigo, 2006). Calpains cause neuronal cell death through various pathways, as indicated by reports that inhibition of calpains prevents neuronal cell death whether it is caused by experimental autoimmune encephalomyelitis, traumatic brain injury, or cerebral infarction (Buki et al., 2003; Hassen et al., 2006).

Cerebral infarction is a life-threatening disease. Cerebral ischemia induces Ca^{2+} influx into neuronal cells, and activates several proteases, including calpains (Neumar et al., 2001; Neumar et al., 2003; Yamashima, 2004). In previous studies, calpain inhibitors have been found to exhibit neuroprotective effects in *in vitro* models of experimental ischemia (Bartus et al., 1994a,b; Li et al., 1998; Markgraf et al., 1998; Farkas et al., 2004; Tsubokawa et al., 2006). As regards brain structures, there are differences among calpain inhibitors in both membrane permeability and affinity, so their efficacies may vary. These differences may be based on the chemical structure, solubility, and ADME (absorption, distribution, metabolism, and excretion) of each calpain inhibitor. For the prevention of neuronal cell death after cerebral ischemia, calpain

inhibitors that are safe, are widely available, and have powerful effects within the brain are needed.

The novel calpain inhibitor ((1S)-1((((1S)-1-benzyl-3-cyclopropylamino-2,3-di-oxopropyl)amino)carbonyl)-3-methylbutyl) carbamic acid 5-methoxy-3-oxapentyl ester (SNJ-1945) has been shown to have good aqueous solubility, good plasma exposure, and good CNS penetration in rats and monkeys (Oka et al., 2006; Shirasaki et al., 2006). Furthermore, administration of SNJ-1945 at 160 mg/kg, i.p. for 14 days produced no obvious toxic signs or abnormalities in rats (Oka et al., 2006). However, there have been no reports on its efficacy against cerebral ischemia. Therefore, in the present study we set out to examine the neuroprotective effects of SNJ-1945 against cerebral infarction in a murine middle cerebral artery occlusion (MCAO) model. To this end, we evaluated adequate doses, therapeutic time-window, and inhibition of calpain activity in the brain after MCAO.

EXPERIMENTAL PROCEDURES

Animal preparation

The experimental designs and all procedures were in accordance both with the U.S. National Institutes of Health Guide for the Care and Use of Laboratory Animals and with the Animal Care Guidelines issued by the Animal Experimental Committee of Gifu Pharmaceutical University. All experiments were performed using male ddY mice (5–6 weeks old, Japan SLC Ltd., Shizuoka, Japan). Every effort was made to minimize the number of animals used and their suffering.

Drugs

SNJ-1945, kindly donated by Senju Pharmaceutical Co. Ltd. (Kobe, Japan), was dissolved in 0.5% carboxymethyl cellulose, and administered intraperitoneally. 2,3,5-Triphenyltetrazolium chloride (TTC), pentobarbital sodium, and isoflurane were purchased from Sigma-Aldrich Co. (St. Louis, MO, USA), Nissan Kagaku (Tokyo, Japan), and Merck Hoei Ltd. (Osaka, Japan), respectively.

Drug treatment

SNJ-1945 was diluted in 0.5% carboxymethyl cellulose. For the evaluation of dose-dependency, mice were injected with SNJ-1945 (10, 30, or 100 mg/kg, i.p.) at 1 h after MCAO. For the evaluation of therapeutic time-window, mice were injected with SNJ-1945 (100 mg/kg i.p.) at 1 h, 3 h, 6 h, or 8 h after MCAO. For Western blot analysis, all mice were injected with SNJ-1945 (100 mg/kg, i.p.) at 1 h after MCAO.

Surgery

Mice were anesthetized with isoflurane 2–3% (for induction) and maintained with 1.0–1.5% isoflurane in 70% N_2O and 30% O_2 via a facemask (Soft Lander; Sin-ei Industry, Saitama, Japan). Focal cerebral ischemia was induced [using an 8–0 nylon monofilament (Ethicon, Somerville, NJ, USA) coated with silicone hardener mixture (Xantpren; Bayer Dental, Osaka, Japan)] via the internal carotid artery, as described by Hara et al. (1996). Briefly, the coated filament was introduced into the left internal carotid artery through the common carotid artery, then advanced up to the origin of the anterior cerebral artery via the internal carotid artery, so as to occlude the middle cerebral artery and posterior communicating artery. At the same time, the left common carotid artery was occluded. Anesthesia did not exceed 10 min.

Physiological monitoring

In all animals during surgery and ischemia, the body temperature was maintained between 37.0 and 37.5 °C with the aid of a heating lamp and heating pad. In randomly selected animals, the left femoral artery was cannulated and blood pressure was measured during the preparation, mean systemic arterial blood pressure (Power Laboratory; AD Instrument, Nagoya, Japan) being measured for 3-min periods starting 10 min before and ending 30 min after MCAO. Arterial blood samples taken 30 min before and 30 min after the induction of ischemia were analyzed for pH and the partial pressures of oxygen (PaO_2) and carbon dioxide ($PaCO_2$) (i-STAT 3G; Abbott Point-of-Care Inc., East Windsor, NJ, USA). Regional cerebral blood flow (CBF) was determined by laser-Doppler flowmetry (Omegaflow flo-N1; Omegawave Inc., Tokyo, Japan) using a flexible 0.5-mm fiber-optic extension to the master probe. The tip of the probe was fixed to the intact skull over the ischemic cortex (2 mm posterior and 6 mm lateral to bregma). Steady-state values obtained after occlusion were expressed as a percentage of the baseline value (obtained at 30 before MCAO).

Analysis of cerebral infarction

At 24 h or 72 h after MCAO, mice were given an overdose of pentobarbital sodium, then decapitated. The forebrain was divided into five coronal 2-mm sections using a mouse brain matrix (RBM-2000C; Activational Systems, Warren, MI, USA). These slices were immersed for 20 min in a 2% solution of TTC in normal saline at 37 °C, then fixed in 10% phosphate-buffered formalin at 4 °C. TTC reacts with intact mitochondrial respiratory enzymes to generate a bright red color that contrasts with the pale color of the infarction. The caudal face of each slice was photographed. The area of the infarction (unstained) in the left cerebral hemisphere was traced and measured using Image J (http://rsb.info.nih.gov/ij/download/), and the infarction volume per brain (mm^3) was calculated from the measured infarction area.

Neurological deficits

Mice were tested for neurological deficits at 24 h or 72 h after MCAO. These were scored as described in our previous study (Hara et al., 1996): 0, no observable neurological deficits (normal); 1, failure to extend the right forepaw (mild); 2, circling to the contralateral side (moderate); 3, loss of walking or righting reflex (severe); 4, dead.

Western blot analysis

Mice were deeply anesthetized and decapitated at the indicated times (6 h or 12 h) after MCAO, and the brain was quickly removed and an 8-mm coronal section cut from the left hemisphere (between 2 and 10 mm from the frontal end of the forebrain). Brain samples were homogenized in 10 ml/g tissue ice-cold lysis buffer [50 mM Tris-HCl (pH8.0) containing 150 mM NaCl, 50 mM EDTA, 1% Triton X-100, and protease/phosphatase inhibitor mixture] and centrifuged at 14,000×g for 40 min at 4 °C. An aliquot of 5 μg of protein was subjected to 10% sodium dodecyl sulfate–polyacrylamide gel electrophoresis, with separated protein being transferred onto a polyvinylidene difluoride membrane (Immobilon-P; Millipore, Billerica, MA, USA). For immunoblotting, the following primary antibodies were used: mouse anti-α-spectrin (nonerythroid) monoclonal antibody (1:1000 dilution; Chemicon, Billerica, MA, USA), cleaved caspase-3 (Asp175) antibody (1:1000 dilution; Cell Signaling, Danvers, MA, USA), monoclonal anti-β-actin (1:1000 dilution; Sigma Aldrich). The secondary antibody was anti-mouse HRP-conjugated IgG (1:2000 dilution). The immunoreactive bands were visualized using SuperSignal West Femto Maximum Sensitivity Substrate (Thermo Scientific, Waltham, MA, USA). The band intensity was measured using a Lumino Imaging

Analyzer (FAS-1000; Toyobo, Osaka, Japan) and Gel Pro Analyzer (Media Cybernetics, Atlanta, GA, USA).

Terminal deoxynucleotidyl transferase-mediated dUTP nick-end labeling (TUNEL) staining

At 24 h after MCAO, mice were deeply anesthetized with pentobarbital sodium, then perfused with 4% paraformaldehyde. Coronal cryostat sections (20 μm) were obtained from frozen brains by serial sectioning. Sections through the striatum were chosen for TUNEL staining. The TUNEL assay was performed according to the manufacturer's instructions (Roche Molecular Biochemicals Inc., Mannheim, Germany). The numbers of TUNEL-positive cells in the cortex and striatum (as the ischemic penumbra) were counted in randomly chosen areas within a high-power field (×400). The histologists (A.K. and Y.N.) were blind as to the group to which each mouse belonged.

Statistical analysis

Data are presented as the means±S.E.M. Statistical comparisons were made using a one-way ANOVA followed by a Student's t-test or Dunnett's test using StatView version 5.0 (SAS Institute Inc., Cary, NC, USA), with $P<0.05$ being considered to indicate statistical significance.

RESULTS

Physiological parameters

There were no significant differences in CBF, mean arterial blood pressure, heart rate, $PaCO_2$, or PaO_2 between the vehicle- and SNJ-1945- (at 100 mg/kg, i.p.) treated groups (Table 1). Surface CBF was reduced to approximately 30% of baseline value immediately after MCAO in all mice.

Dose-dependency

At 24 h after MCAO, an ischemic zone was consistency identified in the cortex and subcortex of the left cerebral

Table 1. Physiological variables before and after MCAO in vehicle-treated and SNJ-1945-treated mice

Parameters	Vehicle	SNJ-1945
Mean blood pressure (mm Hg)		
Before ischemia	78.7±5.6	79.3±4.4
After ischemia	81.9±8.1	81.1±10.5
pH		
Before ischemia	7.33±0.03	7.37±0.02
After ischemia	7.30±0.02	7.32±0.03
$PaCO_2$		
Before ischemia	35.7±3.1	31.7±4.5
After ischemia	33.4±4.9	28.9±4.1
PaO_2		
Before ischemia	168.3±17.2	161.0±11.8
After ischemia	164.0±16.7	163.6±13.7
Regional CBF (%)	33.3±6.8	29.9±2.0

Blood pressure was monitored via the femoral artery. Arterial blood samples were taken 30 min before and 30 min after MCAO, and pH, PCO_2, and PO_2 were measured. Regional CBF values were measured by laser-Doppler flowmetry. There were no significant differences between the vehicle- and SNJ-1945-treated groups. Data are shown as mean±S.E.M. (n=4).

hemisphere. No mice had died at 24 h after MCAO. To judge from the TTC staining results, there was no clear difference between the SNJ-1945- (10 mg/kg, i.p.) and vehicle-treated groups (Fig. 1A and B). However, SNJ-1945 at 30 (Fig. 1C) or 100 mg/kg (Fig. 1D), i.p. (administered at 1 h after MCAO) decreased the cerebral infarction at 24 h after MCAO. By measuring of infarction, SNJ-1945 significantly reduced both the infarct area and volume dose-dependently (Fig. 1E and F). Moreover, SNJ-1945 at 30 and 100 mg/kg, i.p. improved the neurological deficits, but had no such effect at 10 mg/kg (Fig. 1G). A significant effect of SNJ-1945 on infarct area and volume could be seen in the cortex and in the subcortex (Fig. 1H and I), and although dose-dependency was seen in both the cortex and subcortex, it was clearer in the cortex.

Therapeutic time-window

As shown by the TTC staining, SNJ-1945 at 100 mg/kg, i.p., whether administered at 1 h, 3 h, or 6 h after MCAO, decreased the cerebral infarction at 24 h after MCAO (Fig. 2A to D). There was no clear difference between the groups to which SNJ-1945 was given at 8 h after MCAO and the vehicle-treated group (Fig. 2A and E). When administered at 1 h, 3 h, or 6 h after MCAO, SNJ-1945 significantly reduced the infarct area and volume, but had no such effect when administered at 8 h (Fig. 2F and G). If given at up to 6 h after MCAO, SNJ-1945 improved the neurological deficits (Fig. 2H), and the infarct area and volume in the cortex, but administration at 6 h did not have a significant effect in the subcortex (Fig. 2I and J).

Infarction size at 72 h after MCAO

SNJ-1945 (at 100 mg/kg, i.p. administered at 1 h after MCAO) decreased the cerebral infarction (Fig. 3A and B) area and volume measured at 72 h after MCAO (Fig. 3C and D). Moreover, this treatment improved the neurological deficits at 72 h after MCAO (Fig. 3E). Such administration of SNJ-1945 significantly reduced the infarction in both cortex and subcortex (Fig. 3F and G).

TUNEL staining at 24 h after MCAO

The morphological features of TUNEL-stained cells (indicative of the ischemic damage and apoptotic cell death induced by 24 h MCAO) are shown in Fig. 4A to D. The TUNEL method stains fragments of DNA. TUNEL-positive cells displayed either a diffuse staining pattern (Fig. 4E) or a pattern displaying shrunken cell bodies and condensed nuclei (Fig. 4F). These patterns represent necrotic and apoptotic cells, respectively. In the penumbra lesion, TUNEL-positive cells were about 30% fewer in number in the SNJ-1945-treatment group than in the vehicle-treated group in both cortex and subcortex (Fig. 4G).

Western blotting analysis

One of the calpain substrates, α-spectrin, is cleaved to produce a 145 or 150 kDa form, and the amount of cleaved α-spectrin reflects calpain activity. After MCAO, cleaved
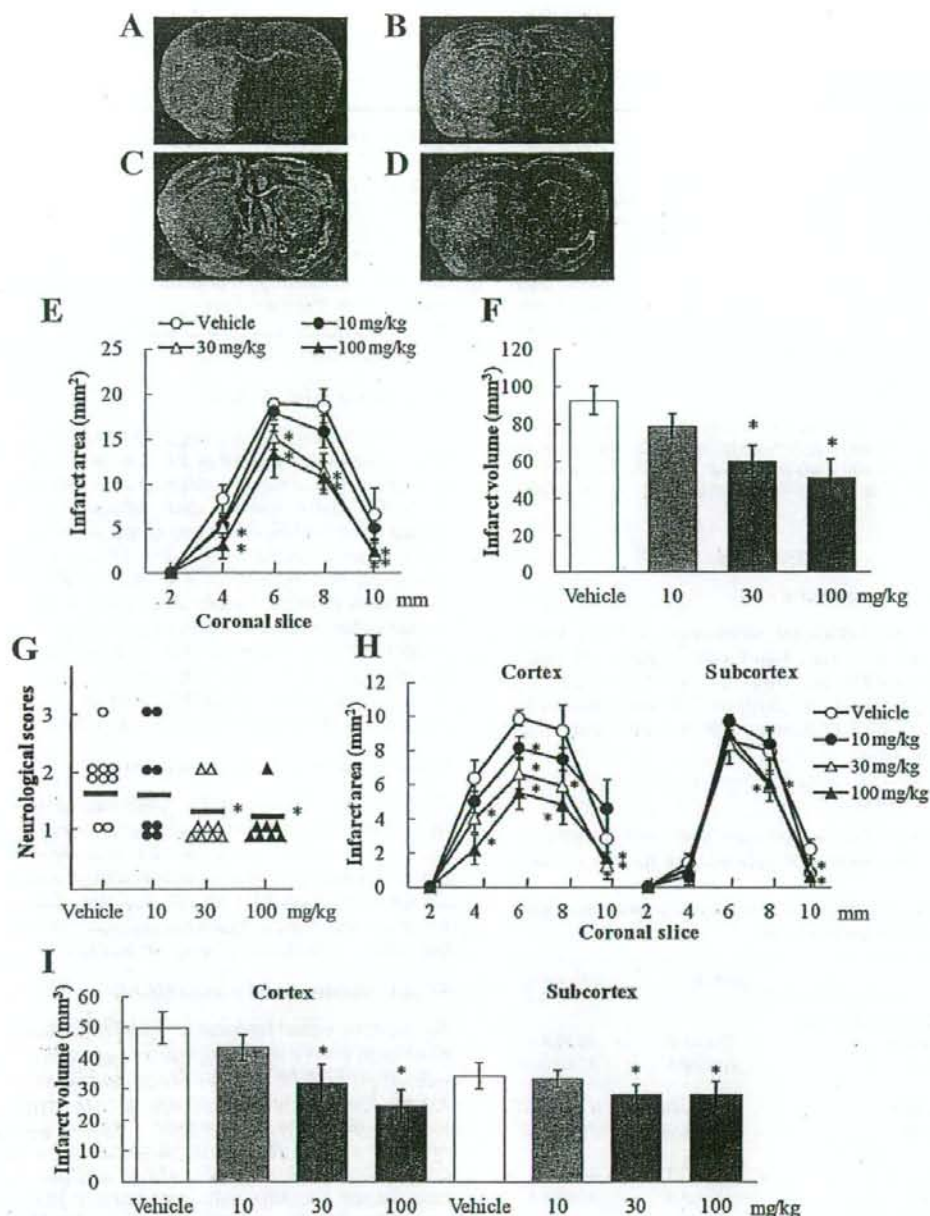
Fig. 1. Effects of SNJ-1945 on infarction at 24 h after MCAO in mice. TTC staining of coronal brain sections (4 mm from olfactory bulb) [(A) vehicle, (B) SNJ-1945 10 mg/kg, i.p., (C) SNJ-1945 30 mg/kg, i.p., (D) SNJ-1945 100 mg/kg, i.p.]. SNJ-1945 decreased infarct area (white area) dose-dependently. (E, F) Effects of SNJ-1945 on brain infarct area (E) and volume (F) measured at 24 h after permanent MCAO. * $P<0.05$ vs. vehicle (Dunnett's test) ($n=8$ or 9). (G) Effects of SNJ-1945 on neurological deficits (assessed at 24 h after MCAO). * $P<0.05$ vs. vehicle (Dunnett's test) ($n=8$ or 9). (H) Brain infarct area in cortex and subcortex at 24 h after MCAO. * $P<0.05$ vs. vehicle (Dunnett's test) ($n=8$ or 9). (I) Brain infarct volume in cortex and subcortex at 24 h after MCAO. * $P<0.05$ vs. vehicle (Dunnett's test) ($n=8$ or 9).

α-spectrin was increased in the ischemic brain hemisphere. SNJ-1945 at 100 mg/kg, i.p. significantly de-

creased the amount of cleaved α-spectrin whether this was measured at 6 h or 12 h after MCAO (Fig. 5A and
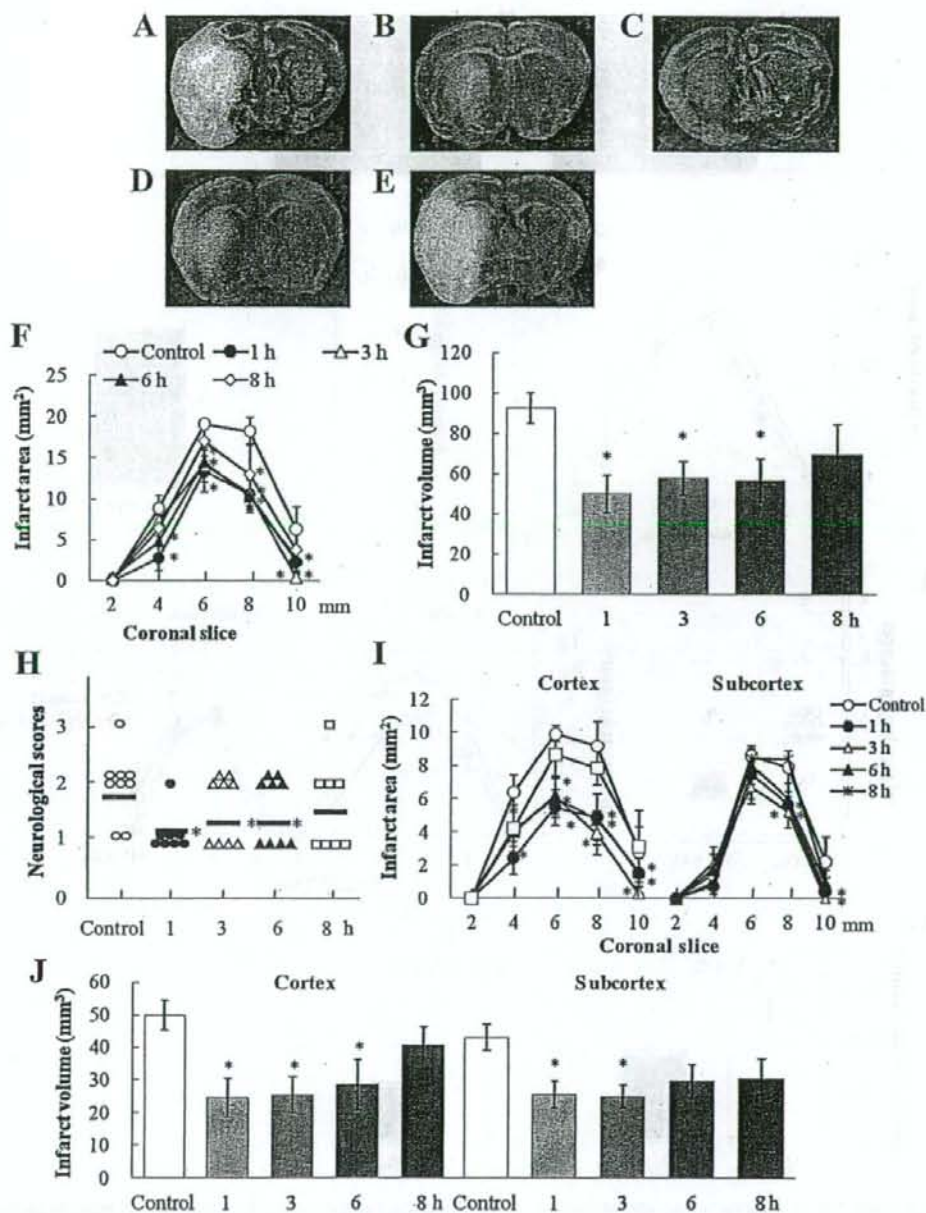
Fig. 2. Effects of SNJ-1945 on infarction at 24 h after MCAO in mice. (A–E) TTC staining of coronal brain sections (4 mm from olfactory bulb) [(A) vehicle was administered at 1 h after MCAO. SNJ-1945 at 100 mg/kg, i.p. was administered at (B) 1 h, (C) 3 h, (D) 6 h, or (E) 8 h after MCAO]. When administered at 1 h, 3 h, or 6 h after MCAO, SNJ-1945 decreased the infarct area (white area). (F, G) Effects of SNJ-1945 on brain infarct area (F) and volume (G) measured at 24 h after permanent MCAO. * $P<0.05$ vs. vehicle (Dunnett's test) ($n=8$ or 9). (H) Effects of SNJ-1945 on neurological deficits (assessed at 24 h after MCAO). * $P<0.05$ vs. vehicle (Dunnett's test) ($n=8$ or 9). (I) Brain infarct area in cortex and subcortex at 24 h after MCAO. * $P<0.05$ vs. vehicle (Dunnett's test) ($n=8$ or 9). (J) Brain infarct volume in cortex and subcortex at 24 h after MCAO. * $P<0.05$ vs. vehicle (Dunnett's test) ($n=8$ or 9).
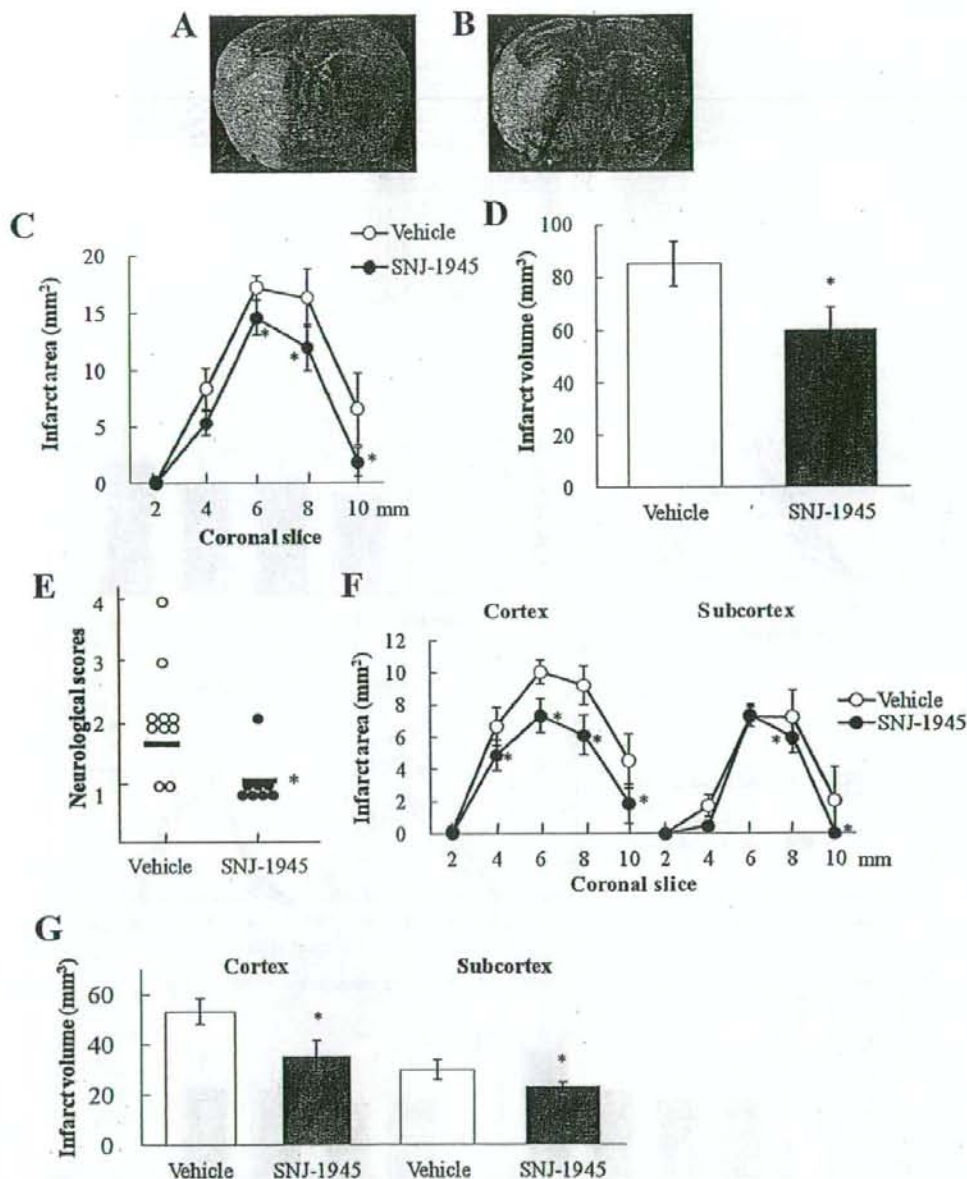
Fig. 3. Effects of SNJ-1945 on infarction at 72 h after MCAO in mice. (A, B) TTC staining of coronal brain sections (4 mm from olfactory bulb). [(A) Vehicle and (B) SNJ-1945 at 100 mg/kg, i.p. at 1 h after MCAO]. SNJ-1945 decreased the infarct area (white area) dose-dependently. (C, D) Effects of SNJ-1945 on brain infarct area (C) and volume (D) measured at 72 h after MCAO. * $P<0.05$ vs. vehicle (Dunnett's test) (n=9 or 10). (E) Effects of SNJ-1945 on neurological deficits (assessed at 72 h after MCAO). * $P<0.05$ vs. vehicle (Dunnett's test) (n=9 or 10). (F) Brain infarct area in cortex and subcortex at 72 h after MCAO. * $P<0.05$ vs. vehicle (Dunnett's test) (n=9 or 10). (G) Brain infarct volume in cortex and subcortex at 72 h after MCAO. * $P<0.05$ vs. vehicle (Dunnett's test) (n=9 or 10).

B), indicating that administration of SNJ-1945 inhibits the calpain activity in the early phase after MCAO.

Caspase-3 is cleaved by calpains to a 17 kDa active form. After MCAO, active caspase-3 was increased within the ischemic lesion at both 12 h and 24 h, but not at 6 h (Fig. 6A and B). SNJ-1945 significantly reduced the amount of active caspase-3 present at both 12 h and 24 h, but not that present at 6 h (Fig. 6B).
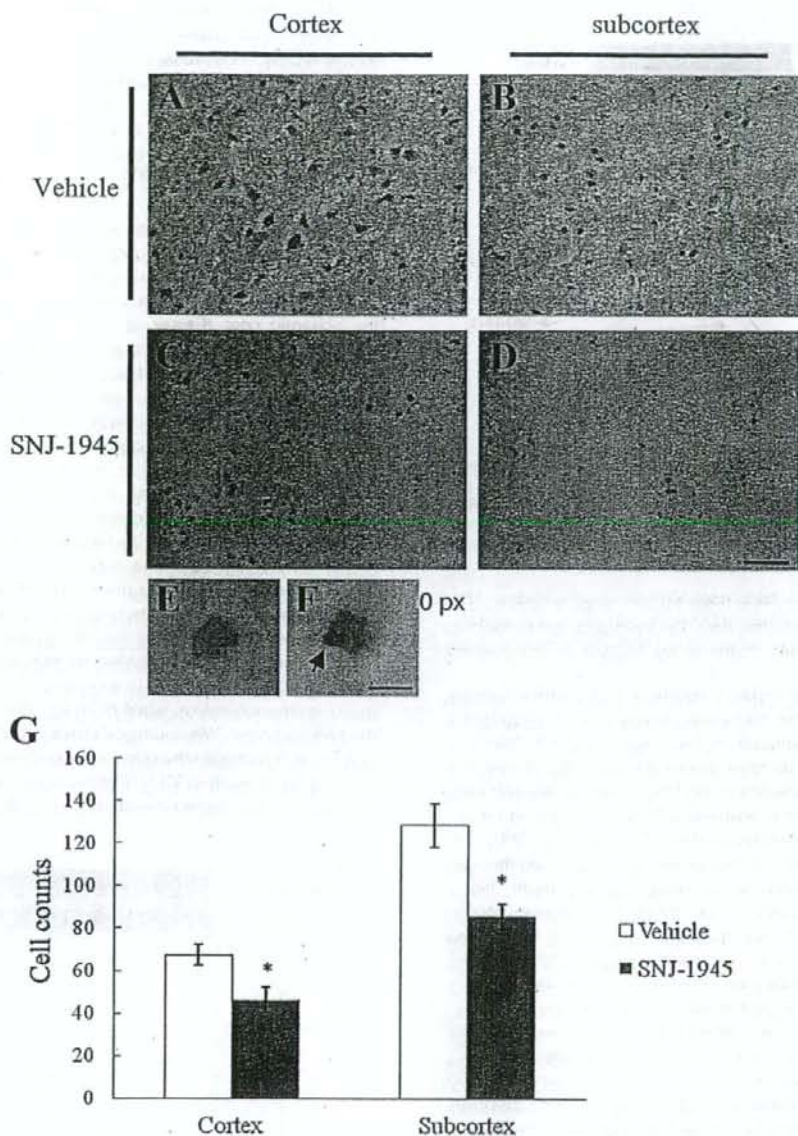
Fig. 4. Effect of SNJ-1945 on TUNEL staining after MCAO in mice. (A–F) TUNEL staining of coronal brain sections (4 mm from olfactory bulb, 20 μm thickness) [(A) vehicle-cortex, (B) vehicle-subcortex, (C) SNJ-1945-cortex, (D) SNJ-1945-subcortex scale bar=50 μm]. (E) "Necrotic cell" and (F) "apoptotic cell" scale bar=10 μm. Necrotic cells appear faint and diffusely stained, while apoptotic cells exhibit apoptotic bodies (arrow). (G) SNJ-1945 reduced the number of TUNEL-positive cells (vs. vehicle) in both cortex and subcortex. * $P<0.05$ (Student's t-test).

DISCUSSION

In the present study, we tested the effects of a novel calpain inhibitor, SNJ-1945, in a murine model of permanent MCAO. When SNJ-1945 was administered at 1 h after MCAO, it exhibited dose-dependent neuroprotective effects, and with doses of 30 and 100 mg/kg reducing both the infarct volume and the neurological deficits signifi-

cantly. Moreover, although SNJ-1945 had its greatest effect when administered at 1 h after MCAO, it also reduced the infarct volume and the neurological deficits when given as late as 3 h or 6 h after MCAO. SNJ-1945 reduced the number of TUNEL-positive cells in the penumbra, while in our Western blotting analysis both calpains and caspase-3 were shown to be activated in the ischemic brain, and
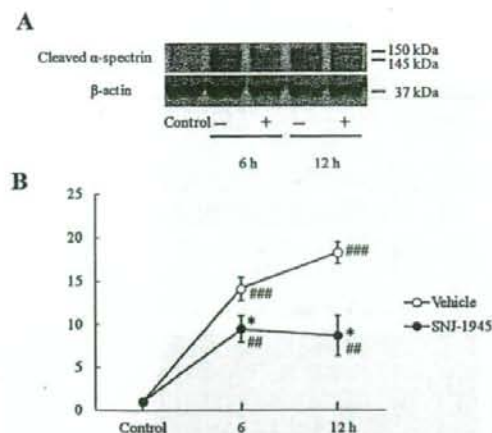
A

Cleaved α-spectrin — 150 kDa / 145 kDa

β-actin — 37 kDa

Control — + — +

6 h   12 h

B

-○- Vehicle
-●- SNJ-1945

Fig. 5. Western blot analysis of cleaved α-spectrin. (A) Cleaved α-spectrin was increased at both 6 h and 12 h after MCAO. (B) Quantitative analysis of Western blotting showed that cleaved α-spectrin was increased, and that SNJ-1945 decreased it, at both 6 h and 12 h after MCAO. ** $P<0.01$, *** $P<0.001$ vs. control (Student's t-test); * $P<0.05$ vs. vehicle (Dunnett's test) ($n=6$).

SNJ-1945 reduced their post-MCAO activity levels. The above data suggest that SNJ-1945 protects neuronal cells against the damage induced by MCAO in the present model.

Markgraf et al. (1998) reported that another calpain inhibitor, MDL28170, had a neuroprotective effect up to 6 h after focal brain ischemia in rats, but not at 8 h. Interestingly, the therapeutic time-window for MDL28170 was the same as that reported here for SNJ-1945. In the ischemic brain, calpains induce neuronal cell death by directly cleaving essential cytoskeletal proteins (Kupina et al., 2003). In fact, calpains are known to activate caspase-3 and thereby cause caspase-3-dependent neuronal cell death. However, Ferrer et al. (2003) found that active caspase-3 could be detected at 4 h after ischemia, but not at 1 h. In the present study, the amount of active caspase-3 in the forebrain was not significantly elevated at 6 h after MCAO, even though its level at this time-point was about 1.5 times control (Fig. 6B). In the early phase of ischemic damage, the direct actions of calpains have greater effects to neuronal cell death than the action of execution caspases such as caspase-3. Furthermore, we found that SNJ-1945 administered at 1 h after MCAO reduced caspase-3 activity at 12 h and 24 h after MCAO (Fig. 6B). Presumably, SNJ-1945 administered at that early time-point after MCAO inhibited calpains, causing the activation of caspase-3 to be inhibited, with a consequent delay in the overactivation of caspase-3 after MCAO. On the other hand, if a calpain inhibitor was administered too late, caspase-3 may have been activated by calpains, and leading DNA-fragmentation. A further point is that active caspase-3 is known to influence upstream events in the mitochondrial apoptotic pathway (Lakhani et al., 2006), and release of cytochrome C or AIF resulting in Bax translocation to the mitochondrial membrane occurs (Cao et al., 2001; Oh et al., 2004; Pol-

ster et al., 2005). Once overactivation of caspase-3 has occurred, the caspase-3 may activate further caspase-3 independently of calpains. In the late phase, the actions of caspase-3 would induce greater neuronal cell death than in the early phase, and so calpain inhibitors will be less effective at preventing neuronal cell death at a late time. Indeed, our data suggest that the "cutoff point" for the effective administration of SNJ-1945 may be around 6–8 h after MCAO.

Ischemia results both in necrosis within the ischemic core and in the activation of signal pathways for cell death and cell survival in the penumbra. In a previous report, apoptosis signals were seen more in the penumbra than in the ischemic core (Ferrer et al., 2003). Since crosstalk between calpains and caspase-3 is involved in one of the apoptotic pathways, inhibition of calpains might have greater effects on neuronal cells in the penumbra than in the ischemic core. In our study, both infarct area and volume were smaller in the cortex than in the subcortex at 24 h or 72 h after MCAO. In our MCAO model, we occluded proximal of MCA, so the ischemic damage was greater in the subcortex and the penumbra lesion was of wider extent in the cortex. On this basis, SNJ-1945 might display greater effects in the cortex.

In the present study, we performed TUNEL staining to evaluate apoptotic cell death. Lei et al. (2004) found in rats that more cells were TUNEL-positive in the penumbra than in the ischemic core at 24 h after MCAO. Moreover, Linnik et al. (1995) reported that apoptotic cell death occurs mainly in the penumbra, while necrotic cell death occurs in the ischemic core. We counted TUNEL-positive cells in the penumbra to evaluate the effect of SNJ-1945 on apoptosis. Our results show that SNJ-1945 reduced TUNEL-positive cells within the penumbra lesion both in the cortex and in
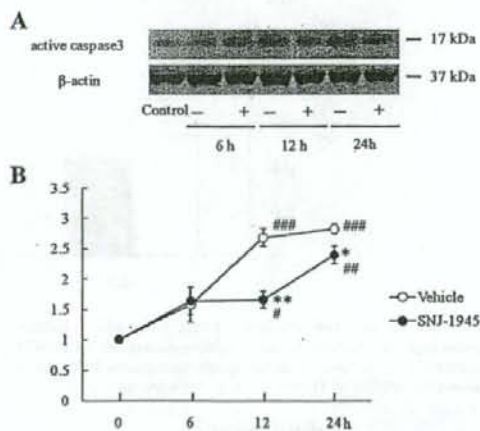
A

active caspase3 — 17 kDa

β-actin — 37 kDa

Control — + — + — +

6 h   12 h   24 h

B

-○- Vehicle
-●- SNJ-1945

Fig. 6. Western blot analysis of active-caspase-3. (A) Active caspase-3 was increased at both 12 h and 24 h after MCAO, but not at 6 h. (B) Quantitative analysis of Western blotting showed that the expression level of active caspase-3 was increased, and that SNJ-1945 decreased it, at both 12 h and 24 h after MCAO. SNJ-1945 had no effect at 6 h. # $P<0.05$, ## $P<0.01$, ### $P<0.001$ vs. control (Student's t-test); * $P<0.05$, ** $P<0.01$ vs. vehicle (Dunnett's test) ($n=6$).

the subcortex (Fig. 4), with more cells being positive in the subcortex than in the cortex. However, reduction of positive-cells by SNJ-1945 was the same in the cortex as in the subcortex (about 30%). So, although ischemic damage was greater in the subcortex in our model, the effect of SNJ-1945 was equal between the cortex and subcortex.

Although some drugs for cerebral infarction are permitted for clinical use, most drugs aim to improve the CBF. These drugs must be administered in the early phase of infarction, otherwise they cause adverse effects. For example, tissue plasminogen activator (t-PA), a most remarkable therapeutic agent for cerebral infarction, should be administered within 3 h after the onset of the infarction and sometimes causes serious complications such as cerebral hemorrhage (Wahlgren et al., 2007). On the other hands, it would appear that SNJ-1945 could save neurons from cell death even if it was given as late as 6 h after the onset of ischemia. Moreover, no obvious side effects have been reported (Oka et al., 2006). The present observations suggest that SNJ-1945 may be a useful therapeutic agent in the treatment of acute cerebral infarction.

CONCLUSION

In conclusion, SNJ-1945 displayed neuroprotective effects in an *in vivo* ischemic stroke model, even when administered as late as 6 h after arterial occlusion. These effects may be, in at least part, based on calpain inhibition and a secondary inhibition of caspase-3.

REFERENCES

Bano D, Nicotera P (2007) Ca²⁺ signals and neuronal death in brain ischemia. Stroke 38:674–676.

Bartus RT, Baker KL, Heiser AD, Sawyer SD, Dean RL, Elliott PJ, Straub JA (1994a) Postischemic administration of AK275, a calpain inhibitor, provides substantial protection against focal ischemic brain damage. J Cereb Blood Flow Metab 14:537–544.

Bartus RT, Hayward NJ, Elliott PJ, Sawyer SD, Baker KL, Dean RL, Akiyama A, Straub JA, Harbeson SL, Li Z (1994b) Calpain inhibitor AK295 protects neurons from focal brain ischemia. Effects of postocclusion intra-arterial administration. Stroke 25:2265–2270.

Bertipaglia I, Carafoli E (2007) Calpains and human disease. Subcell Biochem 45:29–53.

Buki A, Farkas O, Doczi T, Povlishock JT (2003) Preinjury administration of the calpain inhibitor MDL-28170 attenuates traumatically induced axonal injury. J Neurotrauma 20:261–268.

Camins A, Verdaguer E, Folch J, Pallàs M (2006) Involvement of calpain activation in neurodegenerative processes. CNS Drug Rev 12:135–148.

Cao G, Minami M, Pei W, Yan C, Chen D, O'Horo C, Graham SH, Chen J (2001) Intracellular Bax translocation after transient cerebral ischemia: implications for a role of the mitochondrial apoptotic signaling pathway in ischemic neuronal death. J Cereb Blood Flow Metab 21:321–333.

Croall DE, Ersfeld K (2007) The calpains: modular designs and functional diversity. Genome Biol 8:218.

Farkas B, Tantos A, Schlett K, Vilagi I, Friedrich P (2004) Ischemia-induced increase in long-term potentiation is warded off by specific calpain inhibitor PD150606. Brain Res 1024:150–158.

Ferrer I, Friguls B, Dalfó E, Justicia C, Planas AM (2003) Caspase-dependent and caspase-independent signaling of apoptosis in the penumbra following middle cerebral artery occlusion in the adult rat. Neuropathol Appl Neurobiol 29:472–481.

Hara H, Huang PL, Panahian N, Fishman MC, Moskowitz MA (1996) Reduced brain edema and infarction volume in mice lacking the neuronal isoform of nitric oxide synthase after transient MCA occlusion. J Cereb Blood Flow Metab 16:605–611.

Hassen GW, Feliberti J, Kesner L, Stracher A, Mokhtarian F (2006) A novel calpain inhibitor for the treatment of acute experimental autoimmune encephalomyelitis. J Neuroimmunol 180:135–146.

Kupina NC, Detloff MR, Bobrowski WF, Snyder BJ, Hall ED (2003) Cytoskeletal protein degradation and neurodegeneration evolves differently in males and females following experimental head injury. Exp Neurol 180:55–73.

Lakhani SA, Masud A, Kuida K, Porter GA Jr, Booth CJ, Mehal WZ, Inayat I, Flavell RA (2006) Caspases 3 and 7: key mediators of mitochondrial events of apoptosis. Science 311:847–851.

Lei B, Popp S, Capuano-Waters C, Cottrell JE, Kass IS (2004) Lidocaine attenuates apoptosis in the ischemic penumbra and reduces infarct size after transient focal cerebral ischemia in rats. Neuroscience 125:691–701.

Li PA, Howlett W, He QP, Miyashita H, Siddiqui M, Shuaib A (1998) Postischemic treatment with calpain inhibitor MDL28170 ameliorates brain damage in a gerbil model of global ischemia. Neurosci Lett 247:17–20.

Linnik MD, Miller JA, Sprinkle-Cavallo J, Mason PJ, Thompson FY, Montgomery LR, Schroeder KK (1995) Apoptotic DNA fragmentation in the rat cerebral cortex induced by permanent middle cerebral artery occlusion. Brain Res Mol Brain Res 32:116–124.

Markgraf CG, Velayo NL, Johnson MP, McCarty DR, Medhi S, Koehl JR, Chmielewski PA, Linnik MD (1998) Six-hour window of opportunity for calpain inhibition in focal cerebral ischemia in rats. Stroke 29:152–158.

Neumar RW, Meng FH, Mills AM, Xu YA, Zhang C, Welsh FA, Siman R (2001) Calpain activity in the rat brain after transient forebrain ischemia. Exp Neurol 170:27–35.

Neumar RW, Xu YA, Gada H, Guttmann RP, Siman R (2003) Cross-talk between calpain and caspase proteolytic systems during neuronal apoptosis. J Biol Chem 278:14162–14167.

Oh SH, Lee BH, Lim SC (2004) Cadmium induces apoptotic cell death in WI 38 cells via caspase-dependent Bid cleavage and calpain-mediated mitochondrial Bax cleavage by Bcl-2-independent pathway. Biochem Pharmacol 68:1845–1855.

Oka T, Walkup RD, Tamada Y, Nakajima E, Tochigi A, Shearer TR, Azuma M (2006) Amelioration of retinal degeneration and proteolysis in acute ocular hypertensive rats by calpain inhibitor ((1S)-1-(((((1S)-1-benzyl-3-cyclopropylamino-2,3-di-oxopropyl) amino)carbonyl)-3-methylbutyl)carbamic acid 5-methoxy-3-oxapentyl ester. Neuroscience 204:39–48.

Polster BM, Basañez G, Etxebarria A, Hardwick JM, Nicholls DG (2005) Calpain I induces cleavage and release of apoptosis-inducing factor from isolated mitochondria. J Biol Chem 280:6447–6454.

Sanges D, Marigo V (2006) Cross-talk between two apoptotic pathways activated by endoplasmic reticulum stress: differential contribution of caspase-12 and AIF. Apoptosis 11:1629–1641.

Sedarous M, Keramaris E, O'Hare M, Melloni E, Slack RS, Elce JS, Greer PA, Park DS (2003) Calpains mediate p53 activation and neuronal death evoked by DNA damage. J Biol Chem 278:26031–26038.

Shirasaki Y, Yamaguchi M, Miyashita H (2006) Retinal penetration of calpain inhibitors in rats after oral administration. J Ocul Pharmacol 22:417–424.

Sorimachi H, Ishiura S, Suzuki K (1997) Structure and physiological function of calpains. Biochem J 328:721–732.

Tsubokawa T, Solaroglu I, Yatsushige H, Cahill J, Yata K, Zhang JH (2006) Cathepsin and calpain inhibitor E64d attenuates matrix metalloproteinase-9 activity after focal cerebral ischemia in rats. Stroke 37:1888–1894.

Wahlgren N, Ahmed N, Dávalos A, Ford GA, Grond M, Hacke W, Hennerici MG, Kaste M, Kuelkens S, Larrue V, Lees KR, Roine RO, Soinne L, Toni D, Vanhooren G, SITS-MOST Investigators (2007) Thrombolysis with alteplase for acute ischaemic stroke in the Safe Implementation of Thrombolysis in Stroke-Monitor- ing Study (SITS-MOST): an observational study. Lancet 369: 275–282.

Yamashima T (2004) Ca^{2+}-dependent proteases in ischemic neuronal death: a conserved "calpain-cathepsin cascade" from nematodes to primates. Cell Calcium 36:285–293.

Effect of an Inducer of BiP, a Molecular Chaperone, on Endoplasmic Reticulum (ER) Stress-Induced Retinal Cell Death

Yuta Inokuchi,[1] Yoshimi Nakajima,[1] Masamitsu Shimazawa,[1] Takanori Kurita,[2] Mikiko Kubo,[3] Atsushi Saito,[4] Hironao Sajiki,[2] Takashi Kudo,[3] Makoto Aihara,[5] Kazunori Imaizumi,[4] Makoto Araie,[5] and Hideaki Hara[1]

Purpose. The effect of a preferential inducer of 78 kDa glucose-regulated protein (GRP78)/immunoglobulin heavy-chain binding protein (BiP; BiP inducer X, BIX) against tunicamycin-induced cell death in RGC-5 (a rat ganglion cell line), and also against tunicamycin- or N-methyl-D-aspartate (NMDA)-induced retinal damage in mice was evaluated.

Methods. In vitro, BiP mRNA was measured after BIX treatment using semi-quantitative RT-PCR or real-time PCR. The effect of BIX on tunicamycin (at 2 μg/mL)-induced damage was evaluated by measuring the cell-death rate and CHOP protein expression. In vivo, BiP protein induction was examined by immunostaining. The retinal cell damage induced by tunicamycin (1 μg) or NMDA (40 nmol) was assessed by examining ganglion cell layer (GCL) cell loss, terminal deoxyribonucleotidyl transferase (TdT)-mediated dUTP nick-end labeling (TUNEL) staining, and CHOP protein expression.

Results. In vitro, BIX preferentially induced BiP mRNA expression both time- and concentration-dependently in RGC-5 cells. BIX (1 and 5 μM) significantly reduced tunicamycin-induced cell death, and BIX (5 μM) significantly reduced tunicamycin-induced CHOP protein expression. In vivo, intravitreal injection of BIX (5 nmol) significantly induced BiP protein expression in the mouse retina. Co-administration of BIX (5 nmol) significantly reduced both the retinal cell death and the CHOP protein expression in GCL induced by intravitreal injection of tunicamycin or NMDA.

Conclusions. These findings suggest that this BiP inducer may have the potential to be a therapeutic agent for endoplasmic reticulum (ER) stress-induced retinal diseases. (*Invest Ophthalmol Vis Sci.* 2009;50:334–344) DOI:10.1167/iovs.08-2123

Corresponding author: Hideaki Hara, Department of Biofunctional Evaluation, Molecular Pharmacology, Gifu Pharmaceutical University, 5-6-1 Mitahora-higashi, Gifu 502-8585, Japan; hidehara@gifu-pu.ac.jp.

The endoplasmic reticulum (ER) is the cellular organelle in which proteins (destined for secretion or for diverse subcellular localizations) are not only synthesized, but acquire their correct conformation. Perturbations of the environment normally required for protein folding in the ER, or the production of large amounts of misfolded proteins exceeding the functional capacity of the organelle, trigger a pattern of physiological response in the cell, collectively known as the unfolded protein response (UPR).[1–3] The UPR serves to cope with ER stress by transcriptionally regulating ER chaperones and other ER-resident proteins, attenuating the overall translation rate, and increasing the degradation of misfolded ER proteins. ER stress is caused by the accumulation of unfolded proteins in the ER lumen, and it is associated with various neurodegenerative diseases such as Alzheimer's, Huntington's, and Parkinson's diseases, and with type-1 diabetes.[4–6] Recent reports have shown that ER stress is also involved in a variety of experimental retinal neurodegenerative models, such as those of diabetic retinopathy,[7] retinitis pigmentosa,[8,9] and glaucoma.[10,11]

Recently, we reported that BiP expression is upregulated in the retina after intravitreal injection of either tunicamycin or NMDA (a glutamate-receptor agonist).[12,13] Tunicamycin, a glucosamine-containing nucleoside antibiotic, produced by genus *Streptomyces*, is an inhibitor of N-linked glycosylation and the formation of N-glycosidic protein-carbohydrate linkages.[14] Tunicamycin, which reduces the N-glycosylation of proteins, causes an accumulation of unfolded proteins in the ER and thus induces ER stress. Awai et al.[15] previously had demonstrated that NMDA induces CHOP protein (a member of the CCAAT/enhancer-binding protein family induced by ER stress) in GCL and the inner plexiform layer (IPL), and that CHOP^{-/-} mice are more resistant to NMDA-induced retinal cell death than wild-type mice. These findings indicate that ER stress may be involved in these models of retinal injury.

BiP, a highly conserved member of the 70 kDa heat shock protein family, is one of the chaperones localized to the ER membrane,[16,17] and it is a major ER-luminal Ca^{2+}-storage protein.[18,19] BiP works to restore folding in misfolded or incompletely assembled proteins,[20–22] the interaction between BiP and misfolded proteins being dependent on its hydrophobic motifs.[23–25] Proteins stably bound to BiP are subsequently translocated from the ER into the cytosol, where they are degraded by proteasomes.[26,27] Previous reports have show that induction of BiP prevents the neuronal death induced by ER stress.[28–31] Hence, a selective inducer of BiP might attenuate ER stress and be a new, useful therapeutic agent for the treatment of ER stress-associated diseases.

This seemed an interesting idea, and we recently identified BiP inducer X (BIX) while screening for low molecular

mass compounds that might induce BiP using high-through-put screening (HTS) with a BiP reporter assay system (Dual-Luciferase Reporter Assay; Promega Corporation, Madison, WI).[32] We found that BIX preferentially induced BiP mRNA and protein in SK-N-SH cells and reduced tunicamycin-induced cell death. Intracerebroventricular pretreatment with BIX reduced the infarction size after focal cerebral ischemia in mice. In view of the retinal research described above, we wondered whether BIX might reduce the retinal ganglion cell loss and CHOP expression induced by tunicamycin or NMDA treatment.

In the present study, we examined primarily whether induction of BiP might inhibit the retinal cell death induced by tunicamycin in RGC-5 cells in vitro, and/or that induced by tunicamycin or NMDA in mice in vivo.

MATERIALS AND METHODS

All experiments were performed in accordance with the ARVO Statement for the Use of Animals in Ophthalmic and Vision Research, and they were approved and monitored by the Institutional Animal Care and Use Committee of Gifu Pharmaceutical University, Gifu, Japan.

Materials

Dulbecco modified Eagle medium (DMEM) and NMDA were purchased from Sigma-Aldrich (St. Louis, MO). The other drugs used and their sources were as follows: BIX, 1-(3,4-dihydroxyphenyl)-2-thiocyanato-ethanone, was synthesized in the Department of Medicinal Chemistry, Gifu Pharmaceutical University, while tunicamycin was purchased from Wako (Osaka, Japan). Isoflurane was acquired from Nissan Kagaku (Tokyo, Japan) and fetal bovine serum (FBS) was from Valeant (Costa Mesa, CA).

RGC-5 Culture

RGC-5[32] were gifted by Neeraj Agarwal (Department of Pathology and Anatomy, UNT Health Science Center, Fort Worth, TX). Cultures of RGC-5 were maintained in DMEM supplemented with 10% FBS, 100 U/mL penicillin (Meiji Seika Kaisha Ltd., Tokyo, Japan), and 100 μg/mL streptomycin (Meiji Seika Kaisha. Ltd.) in a humidified atmosphere of 95% air and 5% CO_2 at 37°C. The RGC-5 cells were passaged by trypsinization every 3 days, as in our previous reports.[12,13,33] We used RGC-5 without any differentiation.

RNA Isolation and Semi-Quantitative RT-PCR Analysis

To examine the effect of BIX on BiP mRNA expression, RGC-5 cells were seeded in six-well plates at a density of 1.4×10^5 cells per well. After the cells had been incubating for 24 h, they were exposed to 50 μM BIX in 1% FBS DMEM for 0.5, 1, 2, 4, 6, 8, or 12 h, or to 2, 10, 50, or 150 μM BIX in 1% FBS DMEM for 6 h. Total RNA was extracted (RNeasy Mini Kit; QIAGEN KK, Tokyo, Japan) according to the manufacture's protocol. The total RNA was divided into microtubes, and frozen to −80°C. RNA concentrations were determined spectrophotometrically at 260 nm. First-strand cDNA was synthesized in a 20-μl reaction volume using a random primer (Takara, Shiga, Japan) and Moloney murine leukemia virus reverse transcriptase (Invitrogen, Carlsbad, CA). PCR was performed in a total volume of 30 μL containing 0.8 μM of each primer, 0.2 mM dNTPs, 3 U *Taq* DNA polymerase (Promega), 2.5 mM $MgCl_2$, and 1× PCR buffer. The amplification conditions for the semi-quantitative RT-PCR analysis were as follows: an initial denaturation step (95°C for 5 minutes), 20 cycles of 95°C for 1 minute, 55°C for 1 minute, and 72°C for 1 minute, and a final extension step (72°C for 7 minutes). The numbers of amplification cycles for the detection of BiP and β-actin were 18 and 15, respectively. The primers used for amplification were as follows: BiP: 5'-GTTTGCTGAGGAAGACAAAAGCTC-3' and 5'-CACTTCCATAGAGTT-

TGCTGATAATTG-3'; β-actin: 5'-TCCTCCCTGGAGAAGAGCTAC-3' and 5'-TCCTGCTTGCTGATCCACAT-3'.

PCR products were resolved by electrophoresis through 6% (w/v) polyacrylamide gels. The density of each band was quantified using an imaging program (Scion Image Program; Scion Corporation, Frederick, MD).

Real-Time PCR

Real-time PCR (TaqMan; Applied Biosystems, Foster City, CA) was performed as described previously.[34] Single-stranded cDNA was synthesized from total RNA using a high-capacity cDNA archive kit (Applied Biosystems). Quantitative real-time PCR was performed using a sequence detection system (ABI PRISM 7900HT; Applied Biosystems) with a PCR master mix (TaqMan Universal PCR Master Mix; Applied Biosystems), according to the manufacturer's protocol. mRNA expression was measured by real-time PCR using a gene expression product (Assays-on-Demand Gene Expression Product; Applied Biosystems) and a BiP probe (Assay ID Details: Mm00517691). The thermal cycler conditions were as follows: 2 minutes at 50°C and then 10 minutes at 95°C, followed by two-step PCR for 50 cycles consisting of 95°C for 15 seconds followed by 60°C for 1 minute. For each PCR, we obtained the slope value, R^2 value, and linear range of a standard curve of serial dilutions. All reactions were performed in duplicate. The results are expressed relative to the β-actin (Assay ID Details: Mm00661904) internal control.

Cell Viability

To examine the effects of BIX on the cell death induced by tunicamycin (2 μg/mL) or staurosporine (an ER stress-independent apoptosis inducer, 30 nm) RGC-5 cells were seeded at a low density of 700 cells per well into 96-well plates. After pretreatment with BIX for 12 h, tunicamycin or staurosporine was added to the cultures for 48 h or 24 h, respectively. Cell death was assessed on the basis of combination staining with the fluorescent dyes Hoechst 33342 and propidium iodide (PI; Molecular Probes, Eugene, OR) or the change in fluorescence intensity after the cellular reduction of WST-8 to formazan. Hoechst 33342 (λex 350 nm, λem 461 nm) and PI (λex 535 nm, λem 617 nm) were added to the culture medium at final concentrations of 8 and 1.5 μM, respectively, for 30 minutes. Images were collected using a CCD camera (DP30VW; Olympus America, Center Valley, PA) via an epifluorescence microscope (IX70; Olympus, Tokyo, Japan) fitted with fluorescence filters for Hoechst 33342 (U-MWU; Olympus), and PI (U-MWIG; Olympus). In WST-8 assay, cell viability was assessed by culturing cells in a culture medium containing 10% WST-8 (Cell Counting Kit-8; Dojin Kagaku, Kumamoto, Japan) for 3 h at 37°C, with quantification being achieved by scanning with a microplate reader at 492 nm.[35] This absorbance is expressed as a percentage of that in control cells (which were in 1% FBS DMEM) after subtraction of background absorbance.

Animals

Mice used were male adult ddY mice (Japan SLC, Hamamatsu, Japan), male adult Thy-1-cyan fluorescent protein (CFP) transgenic mice (The Jackson Laboratory, Bar Harbor, Maine),[36] and ER stress–activated indicator (ERAI)-transgenic mice carrying the F-XBP1ΔDBD-venus, a variant of green fluorescent protein (GFP) fusion gene, which allows effective identification of cells under ER stress in vivo, as previously described by Iwawaki et al.[37] Briefly, when ER stress in ERAI transgenic mice was induced, splicing of mRNA encoding the XBP-1 fusion gene occurs and the spliced form of F-XBP1ΔDBD-venus fusion gene could be translated into fluorescent protein. Thus, it is visualized by the fluorescence intensity arising from the XBP-Δ-venus fusion protein during ER stress, and we measured it by fluorescence microscopy and immunoblotting in the present study.

All mice were kept under controlled lighting conditions (12 h:12 h light/dark). The mouse genotype was determined by applying standard PCR methodology to tail DNA.

NMDA- or Tunicamycin-Induced Retinal Damage

NMDA- or tunicamycin-induced retinal damage was produced as previously reported by Siliprandi et al. (1992).[38] Briefly, mice were anesthetized with 3.0% isoflurane and maintained with 1.5% isoflurane in 70% N_2O and 30% O_2 via an animal general anesthesia machine (Soft Lander; Sin-ei Industry Co. Ltd., Saitama, Japan). The body temperature was maintained between 37.0 and 37.5°C with the aid of a heating pad. Retinal damage was induced by the injection (2 μL/eye) of NMDA (Sigma-Aldrich) at 20 mM or tunicamycin at 1 μg/mL dissolved in 0.01 M PBS with 5% dimethyl sulfoxide (DMSO). Each solution was injected into the vitreous body of the left eye under the above anesthesia. One drop of 0.01% levofloxacin ophthalmic solution (Santen Pharmaceuticals Co. Ltd., Osaka, Japan) was applied topically to the treated eye immediately after the intravitreal injection. Seven days after the injection, eyeballs were enucleated for histologic analysis. For comparative purposes, nontreated retinas from each mouse strain were also investigated. BIX (0.5 or 5 nmol) or vehicle (5% DMSO in PBS) was co-administered with the NMDA or tunicamycin in each mouse.

Histologic Analysis

In mice under anesthesia produced by an intraperitoneal injection of sodium pentobarbital (80 mg/kg), each eye was enucleated and kept immersed for at least 24 h at 4°C in a fixative solution containing 4% paraformaldehyde. Six paraffin-embedded sections (thickness, 4 μm) cut through the optic disc of each eye were prepared in a standard manner and stained with hematoxylin and eosin. The damage induced by NMDA or tunicamycin was then evaluated, with three sections from each eye being used for the morphometric analysis, as described below. Light-microscope images were photographed, and the cells in the GCL at a distance between 375 and 625 μm from the optic disc were counted on the photographs in a masked fashion by a single observer (Y.I.). Data from three sections (selected randomly from the six sections) were averaged for each eye and used to evaluate the cell count in the GCL.

Retinal Flatmounts and Analysis in Transgenic Mice

Transgenic mice were given an overdose of sodium pentobarbital, and retinas were dissected out and fixed for 30 minutes in 4% paraformaldehyde diluted in 0.1 M phosphate buffer (PB) at pH 7.4. Retinas were subsequently washed with PBS at room temperature, flatmounted on clean glass slides using fluorescent mounting medium (Dako Corp., Carpinteria, CA), and stored in the dark at 4°C for 1 week. The damage induced by tunicamycin was then evaluated, with four sections (dorsal, ventral, temporal, and nasal) from each eye being used for the morphometric analysis, as described below. At various times after intravitreal injections (24 h in ERAI mice and 7 days in Thy-1-CFP transgenic mice), fluorescent images were photographed ($\times$200, 0.144 mm^2) using an epifluorescence microscope (BX50; Olympus) fitted with a CCD camera (DP30VW; Olympus). In the case of Thy-1-CFP transgenic mice, Thy-1-CFP-positive cells at a distance of 1 mm from the optic disc were counted on the photographs in a masked fashion by a single observer (Y.I.). Data from the four parts of each eye were used to evaluate the RGC count.[39]

Immunostaining

Eyes were enucleated as described under Histologic Analysis, fixed in 4% paraformaldehyde overnight at 4°C, immersed in 25% sucrose for 48 h at 4°C, and embedded in optimum cutting temperature (OCT) compound (Sakura Finetechnical Co. Ltd, Tokyo, Japan). Transverse 10-μm thick cryostat sections were cut and placed onto slides (MAS COAT; Matsunami Glass Ind., Ltd., Osaka, Japan). Immunohistochemical staining was performed according to the following protocol: Briefly, tissue sections were washed in 0.01 M PBS for 10 minutes, and then endogenous peroxidase was quenched by treating the sections

with 3% hydrogen peroxide in absolute methanol for 10 minutes, followed by a pre-incubation with 10% normal goat serum. They were then incubated overnight at 4°C with the following primary antibodies: against CHOP (1:1000 dilution in PBS; Santa Cruz, CA), and against BiP/GRP78 (1:1000 dilution in PBS; BD Transduction Laboratories, Lexington, KY). Sections were washed and then incubated with biotinylated anti-rabbit IgG or anti-mouse IgG. They were subsequently incubated with the avidin-biotin-peroxidase complex for 30 minutes, and then developed using diaminobenzidine (DAB) peroxidase substrate. Images were obtained using a digital camera (COOLPIX 4500; Nikon, Tokyo, Japan).

Quantitation of Density

In the DAB-labeled areas of anti-BiP/GRP78 (BD Transduction Laboratories) and anti-CHOP (Santa Cruz) in the GCL and IPL at a distance between 475 and 525 μm (50 $\times$ 50 μm) from the optic disc, retinal DAB-labeled cell density was evaluated by means of appropriately calibrated computerized image analysis, using median density in the range of 0 to 255 as an analysis tool (Image Processing and Analysis in Java, Image J; National Institute of Mental Health, Bethesda, MD) and averaged for two areas.[40] The data lie within the dynamic range of this assays

Briefly, light-microscope images of the above-mentioned areas were photographed, inverted in a gradation sequence using image editing software (Adobe Photoshop 5.5; Adobe Systems Inc., San Jose, CA), and then optical intensity was evaluated using Image J. The score for the negative-control (nontreated with first antibody), as the background value, was subtracted from the scores.

TUNEL Staining

TUNEL staining was performed according to the manufacturer's protocol (In Situ Cell Death Detection Kit; Roche Biochemicals, Mannheim, Germany) to detect the retinal cell death induced by NMDA. Mice were anesthetized with pentobarbital sodium at 80 mg/kg, IP, 24 h after intravitreal injection (either of NMDA 40 nmol/eye or of tunicamycin 1 μg/eye). The eyes were enucleated, fixed overnight in 4% paraformaldehyde, and immersed for 2 days in 25% sucrose with PBS. The eyes were then embedded in a supporting medium (OCT compound) for frozen-tissue specimens. Retinal sections at 10-μm thick were cut on a cryostat at -25°C, and stored at -80°C until staining. After twice washing with PBS, sections were incubated with terminal TdT enzyme at 37°C for 1 h, then washed 3 times in PBS for 1 minute at room temperature. Sections were subsequently incubated with an anti-fluorescein antibody-peroxidase conjugate at room temperature in a humidified chamber for 30 minutes, then developed using DAB tetrahydrochloride peroxidase substrate. Light-microscope images were photographed, and the labeled cells in the GCL at a distance between 375 and 625 μm from the optic disc were counted in two areas of the retina in a masked fashion by a single observer (Y.I.). The number of TUNEL-positive cells was averaged for these two areas, and plotted as the number of TUNEL-positive cells.

Western Blot Analysis

RGC-5 cells were lysed using a cell-lysis buffer (RIPA buffer R0278; Sigma-Aldrich) with protease (P8340; Sigma-Aldrich) and phosphatase inhibitor cocktails (P2850 and P5726; Sigma-Aldrich), and 1 mM EDTA. In vivo, mice were euthanatized using sodium pentobarbital at 80 mg/kg, IP, and their eyeballs were quickly removed. The retinas were carefully separated from the eyeballs and quickly frozen in dry ice. For protein extraction, the tissue was homogenized in the cell-lysis buffer using a homogenizer (Physcotron; Microtec Co. Ltd., Chiba, Japan). The lysate was centrifuged at 12,000g for 20 minutes, and the supernatant was used for this study. Assays to determine the protein concentration were performed by comparison with a known concentration of bovine serum albumin using a BCA protein assay kit (Pierce Biotechnology, Rockford, IL). A mixture of equal parts of an aliquot of